THE UNIVERSITY OF TEXAS AT AUSTIN

ARL-TR-70-44
December 1970

Copy No. 40

TESTS OF VORTEX GENERATORS TO PREVENT SEPARATION OF SUPERSONIC FLOW IN A COMPRESSION CORNER

David K. Gartling

NAVAL AIR SYSTEMS COMMAND
APL/JHU Subcontract 271734, Task B

UNCLASSIFIED

Security Classification

DOCUMENT CONTROL DATA - R & D

Security classification of title, body of abstract and indexing annotation must be entered when the overall report is classified)

1 ORIGINATING ACTIVITY (Corporate author) Applied Research Laboratories The University of Texas at Austin Austin, Texas 78712	2a. REPORT SECURITY CLASSIFICATION UNCLASSIFIED 2b. GROUP —

3 REPORT TITLE

TESTS OF VORTEX GENERATORS TO PREVENT SEPARATION OF SUPERSONIC FLOW IN A COMPRESSION CORNER

4 DESCRIPTIVE NOTES (Type of report and inclusive dates)

technical report

5 AUTHOR(S) (First name, middle initial, last name)

David K. Gartling

6 REPORT DATE December 1970	7a. TOTAL NO. OF PAGES 83	7b. NO. OF REFS 12
8a. CONTRACT OR GRANT NO APL/JHU Subcontract 271734, b. PROJECT NO. Task B c. d.	9a. ORIGINATOR'S REPORT NUMBER(S) ARL-TR-70-44 9b. OTHER REPORT NO(S) (Any other numbers that may be assigned this report) —	

10 DISTRIBUTION STATEMENT

Approved for public release; distribution unlimited.

11 SUPPLEMENTARY NOTES —	12. SPONSORING MILITARY ACTIVITY Naval Air Systems Command Department of the Navy Washington, D. C. 20360

13. ABSTRACT

Tests were made on four vortex generators to determine their ability to prevent flow separation. The generators were of rectangular planform with chord lengths of 0.5 and 1.0 in. and spans of 0.25 and 0.50 in. Generator section shape was a symmetric double wedge. The generators were individually mounted at a 15 deg angle of attack on a flat plate upstream of a 35 deg compression corner. The tests were made in a wind tunnel at an average Mach Number of 4.67. The boundary layer was turbulent and approximately 1/4 in. thick at the test station. Static pressure measurements were taken along the centerline of the plate and on the ramp face. Oil and dye flows and schlieren photographs were used to aid in determining the extent of separation. The vortex generators were found to prevent separation if placed sufficiently close to the compression corner. The unseparated region in each case was very narrow in spanwise extent. Separation was prevented by increasing the momentum of the boundary layer through the action of the tip vortex and a secondary vortex. (U)

DD FORM 1 NOV 65 1473 (PAGE 1)

S/N 0101-807-6801

UNCLASSIFIED

Security Classification

UNCLASSIFIED
Security Classification

KEY WORDS	LINK A		LINK B		LINK C	
	ROLE	WT	ROLE	WT	ROLE	WT
Turbulent Flow						
Separation						
Vortex Generators						
Compressible Flow						
Boundary Layers						

DD FORM 1 NOV 65 1473 (BACK)
(PAGE 2)

UNCLASSIFIED
Security Classification

ARL-TR-70-44
December 1970

TESTS OF VORTEX GENERATORS TO PREVENT SEPARATION OF SUPERSONIC FLOW IN A COMPRESSION CORNER

David K. Gartling

NAVAL AIR SYSTEMS COMMAND
APL/JHU Subcontract 271734, Task B

This work has been sponsored by the Naval Air Systems Command, under Subcontract 271734 with the Applied Physics Laboratory of The Johns Hopkins University

APPLIED RESEARCH LABORATORIES
THE UNIVERSITY OF TEXAS AT AUSTIN
AUSTIN, TEXAS 78712

ABSTRACT

Tests were made on four vortex generators to determine their ability to prevent flow separation. The generators were of rectangular planform with chord lengths of 0.5 and 1.0 in. and spans of 0.25 and 0.50 in. Generator section shape was a symmetric double wedge. The generators were individually mounted at a 15 deg angle of attack on a flat plate upstream of a 35 deg compression corner. The tests were made in a wind tunnel at an average Mach Number of 4.67. The boundary layer was turbulent and approximately 1/4 in. thick at the test station. Static pressure measurements were taken along the centerline of the plate and on the ramp face. Oil and dye flows and schlieren photographs were used to aid in determining the extent of separation. The vortex generators were found to prevent separation if placed sufficiently close to the compression corner. The unseparated region in each case was very narrow in spanwise extent. Separation was prevented by increasing the momentum of the boundary layer through the action of the tip vortex and a secondary vortex.

PREFACE

The separation of a supersonic flow in compression corners is a difficult design problem of modern flight vehicles. The ability to prevent separation would be an obvious aid in the prediction of pressure distributions and heat transfer rates for flight systems. Vortex generators have proved useful in controlling separation in subsonic and transonic flows. This report presents the results of tests of vortex generators to prevent separation of a supersonic flow in a compression corner.

The current study is one of a series, devoted to high speed flow separation and its prevention, conducted at Applied Research Laboratories of The University of Texas at Austin. This work has been sponsored by the Naval Air Systems Command under APL/JHU Subcontract 271734, Task B with the Applied Physics Laboratory, The Johns Hopkins University.

The author would like to express his appreciation to Dr. John C. Westkaemper, Research Engineer, Applied Research Laboratories, for his continued guidance and assistance. Special appreciation is also due Mr. William Creamer and Mr. J. Gary Perser for their assistance in the experimental work.

TABLE OF CONTENTS

LIST OF FIGURES

LIST OF FIGURES (Cont'd)

LIST OF FIGURES (Cont'd)

NOMENCLATURE

α = free interaction angle (see Fig. 1)

AR = aspect ratio

b = vortex generator span

c = vortex generator chord

C_p = coefficient of pressure = $P-P_\infty/q_\infty$

γ = ratio of specific heats = 1.40

ℓ = length

M = Mach Number

P = pressure

q = dynamic pressure

SUBSCRIPTS

∞ = free stream static

o = stagnation or total

s = separation

I. INTRODUCTION

The separation of a viscous fluid flow due to an adverse pressure gradient can present a major problem to the designer of a modern flight vehicle. In the subsonic flight regime, flow separation may cause large modifications in pressure distribution and aerodynamic loading. The supersonic regime adds the problem of high local heating rates to the problem of modified loading. In both cases the performance of an entire flight vehicle system may become dependent on local flow conditions if separation occurs. Since separation causes a variety of design problems, it is useful to investigate the possibilities of preventing separation. The Aeromechanics Division of Applied Research Laboratories of The University of Texas at Austin is conducting an extended investigation of flow separation and its prevention. It is the objective of this report to present the results of experiments using vortex generators to prevent separation of a supersonic turbulent boundary layer in a compression corner.

The separation of a fluid flow in a compression corner is caused by the continued depletion of the kinetic energy of the fluid stream caused by an adverse pressure gradient. Considering the supersonic flow of an inviscid fluid in a compression corner, a single oblique shock wave originating at the corner turns the flow parallel to the downstream wall. When viscosity is included, the inviscid free stream becomes coupled to the viscous boundary layer through a pressure interaction.

Due to viscosity the velocity and kinetic energy of a fluid vary from zero at a solid boundary to the inviscid free stream value at the edge of the boundary layer. At a compression corner the high pressure resulting from the turning of the flow diffuses upstream through the subsonic portion of the boundary layer. The already low energy fluid near the wall is thus forced to expend more energy to overcome the additional pressure force. If the pressure gradient is sufficiently large, the boundary layer will reach a point where it can no longer overcome the pressure force and will separate from the wall.

As shown in Fig. 1 the separation of the flow upstream of a compression corner establishes a new effective geometry for the oncoming flow. At the separation point the flow is deflected through an angle smaller than the original turning angle. This results in a weak oblique shock wave emanating from the separation point. The separated flow reattaches on the downstream wall, where it is turned parallel to the wall through a second oblique shock wave. Between the separated fluid and the compression corner a low speed vortical flow is established by the free shear action of the boundary layer and the upstream directed pressure gradient.

The fundamental aspects of flow separation have been investigated by numerous workers with a view toward correlating separation parameters with local flow conditions (Ref. 1,2,3). In the area of preventing separation the majority of the work has been in the subsonic and transonic speed regimes. During the late 1940's and early 1950's workers

at United Aircraft Company demonstrated the use of vortex generators to prevent separation, primarily in subsonic flows. British investigators during the late 1950's extended the use of vortex generators to the transonic flight regime (Ref. 4,5).

The mechanism by which separation was prevented in these cases consisted of re-energizing the low momentum boundary layer. By placing a number of small, wing-shaped vanes or generators normal to the surface, a system of streamwise vortices is produced. The vortex motion sweeps high momentum fluid from the free stream into the low momentum boundary layer as the vortex system proceeds downstream. If the boundary layer momentum is increased sufficiently, the adverse pressure gradient will be overcome and separation prevented.

The utility of vortex generators in preventing separation in subsonic and transonic flows has been demonstrated. Some previous work done at Applied Research Laboratories of The University of Texas at Austin was directed toward extending the use of vortex generators to supersonic flows. Whitten in Ref. 6 measured the drag of several generator shapes but did not demonstrate their use in preventing separation. The work of the present report was undertaken to obtain a better definition of the flow behind a vortex generator placed upstream of a compression corner.

The experimental program consisted of two main phases. The first phase consisted of defining the separation geometry produced by the compression corner. This was accomplished through the use of static pressure measurements, oil and dye flows, and schlieren photographs.

The remainder of the experimental work concentrated on determining the effect of a single vortex generator on the separation region, using the same techniques as in the first phase.

II. EXPERIMENTAL APPARATUS AND PROCEDURE

A. Wind Tunnel

The tests were performed in the 6 x 7 in. wind tunnel of Applied Research Laboratories of The University of Texas at Austin. This is a blow-down type facility with a nominal Mach Number of 5.0 provided by fixed, two-dimensional nozzle blocks. The average Mach Number for the test program was 4.67. The stagnation pressure varied from 265 to 270 psia during the test program, but was controlled automatically to within ±3 psi during any particular test. The stagnation temperature range for this program was 162° to 179°F, with an average of 176°F. This was sufficient to prevent moisture condensation in the wind tunnel. For each particular test the supply air was heated to the preset value using electric resistance heaters located upstream of the stilling chamber. The stagnation temperature was constant within ±5°F during any one test.

B. Flat Plate and Ramp

The tests were conducted with the flat plate, ramp combination shown in Fig. 2. The plate was made from 3/4 in. thick aluminum and was 17.50 in. long and 6 in. wide. A sharp leading edge was provided by a 12.5 deg chamfer machined on the side opposite the test surface. A boundary layer tripper strip, made of 80-grit emery cloth, was mounted approximately 1/2 in. from the leading edge.

The ramp was made from mild steel and machined to provide a 35 deg turning angle from the flat plate. The ramp test face was 1.08 in. long and rose 0.625 in. above the plate surface. When mounted on the plate, the turning corner was 13.2 in. from the leading edge. A rubber sealant was used to provide an airtight joint at the ramp-plate interface.

The plate was mounted horizontally between the sidewalls of the wind tunnel, with the test surface coincident with the nozzle center-plane. A rubber gasket was placed between the model and wind tunnel wall to prevent air flow through the mounting-clearance gap.

The model contained static pressure taps arranged in a centerline and spanwise pattern (Fig. 2). The taps were spaced every 1/2 in. along the centerline of the flat plate from a point 7.65 in. upstream of the ramp to a point 4.65 in. from the ramp. From that point to the ramp the tap spacing was 1/16 in. The quantity of taps on this portion of the model proved more than necessary for this study. Thus, only alternate pressure taps, beginning with the first, were used. This gave a pattern of measurements taken 1 in. apart from 7.65 in. to 4.65 in. upstream of the ramp, and 1/8 in. apart from 4.65 in. to the ramp (Fig. 3). A centerline pattern on the ramp provided taps 0.1 in. apart beginning 0.1 in. from the compression corner. The spanwise pattern consisted of three rows of taps located 0.3 in., 0.6 in., and 0.9 in. from the compression corner. Each row extended 1 in. on both sides of the centerline with taps spaced 0.1 in. apart in each row (Fig. 3).

The plate was also fitted with a thermocouple, located ahead of the separation region, to monitor plate temperature. A recess machined in the back of the plate and ramp provided space for the pressure and thermocouple leads. A cover plate provided protection to this area from the free stream flow.

The flat plate was provided with three slots for the mounting of the vortex generators. The centerline of the forward slot was located 4.9 in. upstream of the ramp on the centerline of the model. The centerlines of the remaining two slots were located 2.5 in. upstream of the ramp. One of these slots was located 3/16 in. to the right of the centerline and the other slot was 1/2 in. to the left of the centerline (Fig. 3). All three slots were inclined at a 15 deg angle to the plate centerline to provide the vortex generators with an angle of attack. The fourth slot seen in Fig. 2 was not used in this investigation.

C. Vortex Generators

The vortex generators are shown in Fig. 4 and their dimensions and designations are given in Table I. The generators were made of mild steel and were all of rectangular planform. Four different generators were used, with chord lengths of 0.5 and 1.0 in. and spans of 0.25 and 0.50 in. The section shape of each generator was a symmetric double wedge with the maximum thickness of 0.064 in. occurring at the mid-chord point. Each generator was provided with a mounting tab 3/8 in. long, 1/16 in. wide, and 1/4 in. deep. The generator was mounted in the desired slot on the plate using a thermoplastic adhesive, Crystalbond 509. All of the generators were mounted at an angle of attack of 15 deg.

D. Flow Visualization Techniques

Extensive use was made of various flow visualization techniques to help define the flow patterns. Schlieren photographs were taken of each configuration, using a single-pass schlieren system. The light source was a tungsten, ribbon-filament lamp. This system allows either black and white or color photographs, though in this program color was used exclusively due to its increased definition.

A dye injection technique was also used to define the flow on the plate surface and ramp face. An oil soluble dye dissolved in naptha was injected through a pressure orifice using the pressure differential between the inside of the wind tunnel and the atmosphere.

Due to the large velocities present in the flow, the dye injection proved to be of limited value and subsequently an oil flow technique was employed. A mixture of 30 weight motor oil and titanium dioxide powder proved satisfactory. The oil was daubed on the plate, the tunnel started, and the pattern allowed to form. However, as in the case of the dye injection, the entraining nature of the flow caused buildups of oil and dye. Upon shutdown of the tunnel, the pattern was distorted by the flow of excess oil. Since the tunnel geometry precluded use of photographic equipment during operation, the patterns were observed and sketches made during each run.

E. Instrumentation and Procedure

The model static pressures were displayed on three multitube mercury manometer boards and were recorded photographically. The plate thermocouple output was recorded on a Honeywell-Brown strip chart

recorder, as was the output of the wind tunnel stagnation temperature thermocouple. The stilling chamber pressure was monitored with a bourdon type pressure gauge which was recorded photographically.

For any particular test the stilling chamber pressure and temperature controllers were set to predetermined values. The tunnel was then started and the stagnation pressure allowed to stabilize before the static pressures were recorded. Since the plate was not heated to recovery temperature prior to each run, the plate temperature was monitored periodically. The preselected stagnation temperature made the recovery temperature approximately 118°F. Due to the usually high ambient temperature (approximately 80-90°F), the temperature difference between the plate at the start of a run and the recovery temperature was small. As a result of the short run times (approximately 25 sec), the plate temperature increased less than 10°F during the runs monitored. This was felt to be representative of the entire test program, making the study nearly adiabatic. During the early phases of the testing at least four duplicate runs were made on each configuration. Good repeatability during this phase allowed the number of runs per configuration to be reduced to two in the later stages of the program.

III. [illegible]

A. Data Reduction

The static pressure data were reduced by a computer program written for the University of Texas at Austin CDC 6600 computer. For each run the stilling chamber pressure, atmospheric pressure, and manometer board readings were entered as data for the program. The computation procedure began by calculating the free stream conditions, using the average of three static pressures from taps located upstream of the forward generator slot. From this value and the input value of stagnation pressure, the free stream Mach number was determined using

$$\frac{P_\infty}{P_0} = \left[1 + \frac{\gamma-1}{2} M_\infty^2\right]^{-\gamma/\gamma-1} \quad , \tag{1}$$

where $\gamma=1.4$. The dynamic pressure was then calculated from the equation

$$q_\infty = \frac{\gamma}{2} P_\infty M_\infty^2 \quad . \tag{2}$$

Each static pressure reading was then nondimensionalized using the equation

$$C_p = \frac{P-P_\infty}{q_\infty} \quad . \tag{3}$$

The pressure coefficients and corresponding tap locations were then printed as output.

Some measurements were also made using the schlieren photographs. Separation lengths and shock wave angles were measured by projecting the 35mm slides on a screen and using a Gerber Variable Scale and a protractor.

B. Accuracy

The static pressures were displayed on three mercury manometer boards having least scale divisions of 0.2 and 0.1 in. The photographic records were found to be of sufficient clarity to allow interpolation to 0.05 in. Due to the low pressures being recorded, an error in manometer reading of ±0.05 in. corresponds to an error of 6.6% in static pressure. However, by reduction of the data to coefficient form, the variation in C_p was less than ±0.01, which was deemed sufficient for this study.

IV. RESULTS AND DISCUSSION

The phenomenon of separation is highly dependent on the type of boundary layer present and the magnitude of the pressure gradient retarding the flow. A turbulent boundary layer was assumed for this program based on the presence of a boundary layer trip and a calculated Reynolds Number per foot of 14×10^6. The boundary layer was approximately 1/4 in. thick in the test area as deduced from the schlieren photographs.

A. Separation Region without Generators

The centerline and spanwise pressure distributions obtained for the compression corner without the generators are plotted in coefficient form in Fig. 5(a) and (b).

1) Separation Parameters

The centerline pressure profile shown in Fig. 5(a) is typical of the separation profile for a two-dimensional turbulent boundary layer. The point of separation is generally taken to be the first inflection point in the pressure profile. This occurs 1.375 in. upstream of the compression corner. Reattachment of the flow on the downstream wall corresponds to the third inflection point in the profile, which is 0.458 in. along the ramp face. The middle inflection point is the plateau pressure rise, which is due to the deflection of the external stream. The plateau pressure coefficient and the location of separation and reattachment are sufficient to allow calculation of several separation parameters.

The free interaction angle or angle between the free stream direction and the dividing streamline at separation was obtained by two methods. The plateau pressure coefficient and free stream Mach Number permitted use of the oblique shock relations or the charts of Ref. 7 to obtain the corresponding deflection angle. This method yielded a free interaction angle of α=8.75 deg. By use of the ramp geometry and the location of separation and reattachment, a free interaction angle of α=8.55 deg was calculated. Measurements from schlieren photographs (Fig. 6) showed a turning angle of approximately α=10 deg, verifying the calculations.

The separation length (Fig. 1) was found by trigonometry using the free interaction angle and the location of separation and reattachment. This yielded a value of l_s=1.77 in., while schlieren photographs showed l_s=1.9 in. A comparison of these values for free interaction angle and separation length with data obtained by Gillette (Ref. 3) showed good agreement. A comparison of centerline pressure distributions with those obtained by Gillette, and Sterrett and Emery (Ref. 8) also showed good agreement.

It should be noted that the peak pressure on the ramp falls short of that predicted by inviscid theory. This phenomenon has been noted by a number of investigators and is attributed to the presence of the sidewalls. The low speed reverse flow region of separation is prevented from spanwise venting by the sidewalls. This causes a larger separation area than for an unbounded flow. The result is a larger

free interaction angle, a stronger shock wave at separation, and a smaller final pressure rise. Work by Kaufman, et al. (Ref. 9) supports this hypothesis

2) Three-Dimensional Effects

The spanwise pressure distributions plotted in Fig. 5(b) show the three-dimensional effects in the flow. Spanwise variations in pressure were observed on the ramp face, indicating a nonuniform flow. To aid in determining the character of the flow, a series of oil and dye flow tests was made. The flow pattern obtained from these tests is sketched in Fig. 7. The separation line was essentially straight over approximately 60% of the center portion of the plate. Near the sidewalls the separation line became curved and joined the curved separation line of the sidewall boundary layer. In the center portion of the plate the flow in the separated region was directed uniformly upstream. Close to the sidewalls a spanwise velocity component, directed outward from the centerline, caused a curvature of the streamlines, which culminated in a surface vortex at the separation line near each sidewall.

In the reattachment region on the ramp face, a series of regularly spaced radial flow patterns was noted. The centers of each pattern were located at the reattachment line and were spaced at 1 in. intervals in the spanwise direction. From each center the flow was radial in all directions. At a small distance from the center the flow became more streamwise, resulting in highly curved streamlines. At the spanwise points where two patterns joined, a heavier oil flow resulted giving the appearance of a striation pattern. This striation of the

flow was more noticeable downstream of reattachment than in the separated region, where the oil pattern was less distinct.

The presence of similar spanwise striations has been observed by several investigators using various geometries. Ginoux (Ref. 10) in an investigation of laminar reattachment observed regular striations that were accompanied by regular variations in pressure and heat transfer rates. Gillette (Ref. 3) and Roshko and Thomke (Ref. 11) noted similar patterns for turbulent reattaching flows. The cause of the striations is generally attributed to the creation of small streamwise vortices in the boundary layer, due to the turning of the flow at separation and reattachment. These Görtler-type vortices are considered three-dimensional perturbations on an otherwise two-dimensional flow. Based on the straightness of the separation line and the agreement of the calculated separation parameters with those of other investigators, the flow for this test program was deemed typical of separated flows resulting from compression corners.

B. Configurations with Generators

A few introductory comments on the vortex generator configurations and results are in order. The principle by which separation is prevented in the subsonic case is based on the vortex produced at the generator tip. In the supersonic case the tip vortex is accompanied by a complex system of shock and expansion waves from the generator body. This results in a region of velocity and pressure variation downstream of the generator, which is indistinguishable from the tip vortex in the measurements made in this investigation. The experimental results and

conclusions of this report are thus based on the effect of the total generator "wake" on the separation area. Also, as the flow pattern created by the generator wake and separation region is extremely complex, a detailed analysis is beyond the scope of the present work. Therefore, only a qualitative description of the main features of the flow are presented in the following sections.

General practice in separation studies is to rely on centerline pressure distributions to determine the nature and extent of separation. This practice is sufficient when the flow is at least quasi-two-dimensional. However, during the present investigation it became evident that the centerline profile was inadequate to determine the extent of separation in the presence of a vortex generator. The spanwise pressure distributions were essential in defining the region affected by the generators and in providing insight into the mechanism by which separation is prevented. Static pressure measurements alone were not sufficient to determine whether separation had been prevented, since no prior criteria were available for comparison. By the extensive use of oil flows, a surface pattern for each configuration was defined. These patterns were then correlated with the pressure profiles to determine the predominate features of the flow. It should be remembered that the oil flows indicate flow near the surface, and extrapolation upward through the boundary layer is not valid. To aid in visualizing the flow in the free stream region a simplified inviscid shock expansion analysis was made for each generator section shape. Using the oil flow and inviscid analysis as guides, a heuristic description for each configuration was developed.

1) Forward Location

The pressure distributions for the four generators in the forward location are shown in Figs. 8 to 11. The centerline profile for each generator shows a slight lowering of the plateau pressure though the profile shape remains similar to the typical separation profile.

In the spanwise profiles all of the generators showed some deviation from the no-generator profile. Generators 1 and 4 had similar patterns though they differed in the magnitude of the variations. In both cases the downstream development of two pressure peaks on either side of the centerline was noted. Separating each peak and outboard of the peaks were regions of low pressure. Generator 1 showed a more distinct development of these variations than did the smaller chord generator 4. However, in neither case were the changes in pressure coefficient greater than 0.2 from the no-generator values.

Generators 2 and 3 also showed a similarity in spanwise profiles, though again the magnitude of the variations was proportional to chord length. For the short span generators a single pressure peak developed to the leeward side of the generator. This peak was noted to be unsteady for generator 2. To the windward side of the generators a very low pressure region developed.

The sketch of the oil flow patterns obtained for these configurations is shown in Fig. 12. None of the flow tests showed a flow of oil streamwise over the entire ramp face, indicating separation was not prevented by the generators in this forward location. The basic

pattern in Fig. 12 was common to all four generators, with only the position of the surface vortex varying from one generator to another. For generators 1 and 4 the pattern was as shown in Fig. 12; for generators 2 and 3 the vortex was centered on the model centerline.

Common to all four configurations is the low pressure area near the centerline in the spanwise profiles. The shock expansion analysis for the portion of the generator in the free stream indicated velocities at the trailing edge comparable to free stream velocity. At the outer edge of the boundary layer, the high velocity flow would intersect the ramp at the reattachment line or higher. Since the largest variations in pressure appear high on the ramp, it is felt that the pressure trough in the profile is a result of the high velocity flow off the trailing edge of the generator.

The flow near the surface also has a relatively high velocity region at the trailing edge but is complicated by the presence of a streamwise vortex and the separation area. In the corner formed by the windward side of the generator and the plate, a streamwise vortex is formed due to the nonuniform turning of the boundary layer by the generator. Near the surface the slower moving fluid is turned through a greater angle than the faster moving flow at the outer edge of the boundary layer. The result is a "twisting" of the boundary layer and the formation of a streamwise vortex near the surface (Ref. 12). This vortex acts to increase the momentum of the fluid near the surface at the generator trailing edge. As seen in the oil flow, the fluid in this region has sufficient momentum to penetrate the separation region causing a cusp in the separation line. However, with the generator

relatively far upstream the adverse pressure gradient is still sufficient to eventually retard the flow, causing separation. The farthest point of attached downstream flow is marked by the downstream edge of the surface vortex seen in the oil flow.

The pressure peaks which were measured on the ramp face are associated with the shock wave system created by the leeward side of the generator. For generators 2 and 3 the pressure peak is quite evident. From its spanwise location it appears this peak is the result of the trailing edge shock wave. The oil flow clearly shows the location of the trailing edge shock up to the point of separation. At separation the nature of the flow at the plate surface and at the outer edge of the boundary layer becomes distinctly different. Above the separated region the flow is nominally that of the free stream. The trailing edge shock wave can therefore proceed downstream to an intersection with the ramp. However, in the separated region where the velocities are substantially lower, the trailing edge shock is dissipated. These suppositions are supported by the streamwise location of the pressure peaks on the ramp. The largest peaks occur high on the ramp, which reflects the free stream and reattached boundary layer flows. The smaller peaks, indicating a weak shock, occur low on the ramp in the separated area.

The unsteadiness noted in the peak pressures for generator 2 and the relatively small peaks for generator 3 are believed to be the result of the interaction of the tip vortex and the trailing edge shock wave. The small chord and slightly larger shock wave angles of generator 3 cause the tip vortex and trailing edge shock to intersect further

upstream than for the longer generator 2. It is thought that the intersection of the vortex and shock wave results in an attenuation of the pressure variations associated with each. The reduced pressure peak for generator 3 indicates the interaction is essentially complete, while for generator 2 the process is still occurring at the ramp area as indicated by the unsteadiness in pressure.

The pressure peaks observed for generators 1 and 4 are much smaller in magnitude than those of the shorter span generators. As a result of the longer span, both generators are in a large free stream environment. The elevation of the generator tip results in the stronger tip vortex being carried downstream above the viscous layer. It is believed that the induced velocities from this vortex cause a lateral shift in the trailing edge shock wave. This shift is very evident in the spanwise pressure profiles for generator 1 (Fig. 8(b)). Here the pressure peak is to the windward side of the generator instead of the leeward side, as in the case of the short span generators. The lateral shift is also noticeable in the surface vortex at the base of the ramp. The tip vortex again causes an attenuation of the trailing edge shock wave, with the smaller chord generator being affected more. The character of the flow near the surface is essentially the same as that downstream of the short span generators.

2) Aft Locations

The pressure distributions for the aft location with the generator to the right of the centerline are plotted in Figs. 13 to 16.

After reviewing the results of this test location, a lateral shift in generator location was made to obtain measurements over a larger portion of the wake. The resulting pressure distributions for the generator in the aft location to the left of the centerline are shown in Figs. 17 to 20. A comparison of the results from these two lateral locations show the expected shift in wake profiles with little variation in pressure magnitudes. The longitudinal pressure distributions are quite different since they are taken at two different lateral positions with respect to the generator wake. Since the location to the left of the centerline covers the largest extent of the generator wake, the following discussion will be based primarily on that position.

All of the centerline profiles in Figs. 17 to 20 show considerable variation from the no-generator results. Generators 1, 2, and 4 display profiles that have no well defined plateau pressure or other features of a typical separation profile. Near the base of the step there is a region where the pressure rises to a small peak before a sharp rise to the maximum C_p value. This indicates a small locally separated area with a short separation length and a large free interaction angle. Generator 3 shows a typical separation profile but has a reduced peak pressure and no extended plateau pressure region. Near the location of each generator the centerline pressure rise to a small peak and returns to near the undisturbed value. The leading edge shock wave from the generator is believed to cause this pressure peak.

The speed profiles for the four generators are similar in shape, with only the magnitude of the variables being different. In each case there is a streamline development of two pressure peaks separated by a low pressure region. The peaks are well defined for generators 1, 2, and 4, while generator 3 has one strong peak and another weaker one.

The oil flow patterns associated with this location are sketched in Figs. 21 to 24. In each case there was a region in which the flow was not separated, as indicated by a flow of oil over the rear face. The extent to which separation was prevented was indicated by the relative width of the oil flow on the rear. In this respect generator 2 was the most effective, while generators 1, 4, and 3 followed in that order.

The flow pattern with the generator in the aft location is substantially different from the forward location, though the mechanism by which the pattern is fixed is the same. Near the middle division of the generator trailing edge, the streamline vortex pattern on the windward side of the generator side mounts to the flow. This high velocity fluid stream has sufficient momentum to overcome the pressure gradient caused by the rear. This results in a locally attached flow over the rear with a corresponding trough in the spanwise pressure profile. Outward from this region as the generator effect decreases, surface eddies are formed by the shear forces between the attached (downstream) and separated (upstream) flow. The location and direction

of rotation of these vortices seem to be dependent on aspect ratio and the trailing edge conditions for each generator. For generator 2, with the lowest aspect ratio, the vortices rotate in opposite directions. The remaining generators have co-rotating surface vortices and higher aspect ratios. The oil flow for generator 1 indicates a stalled condition at the trailing edge, while for generator 4 the pattern indicates the onset of stall. In these two cases the surface vortex to the leeward side of the generator was further upstream than for the unstalled generators. Stalling on generators 1 and 4 was believed to be the result of the high downstream pressure, the long span of the generators, and the high angle of attack.

At the outer edge of the boundary layer the generator is influencing a free stream flow. The shock wave system from the generator is thus able to proceed downstream above the separated area and intersect the ramp. The two pressure peaks indicated in the spanwise profiles correspond to the leading and trailing edge shock waves. In this aft location there appears to be little effect due to the tip vortex, perhaps because of the reduced streamwise distance over which the vortex has to act. Outboard of each pressure peak the pressure tends toward the no-generator values, indicating the narrow region affected by the generator.

In Fig. 25 is shown a schlieren photograph of generator 1 in the aft location. Note that the shock wave emanating from the separation point is no longer a single compression wave as in the no-generator

configuration. The breakdown of the single shock wave into several compression waves is felt to be the result of the highly curved separation line near the generator shock waves. Due to the narrow spanwise extent of the unseparated region, schlieren photographs did not show any detail in this area. The photograph of Fig. 25 was typical of those for generators in the aft location.

V. SUMMARY AND CONCLUSIONS

An experimental investigation was made to determine the usefulness of vortex generators in preventing the separation of a supersonic flow in a compression corner. The vortex generators were mounted on a flat plate at two stations upstream of a 35 deg ramp. The average Mach Number was 4.67 and the Reynolds Number was 14 million per foot. The boundary layer on the plate was turbulent and approximately 1/4 in. thick. Static pressure measurements, oil and dye flows, and schlieren photographs were used to develop a qualitative description of the flow.

The following conclusions were made:

1) A vortex generator, if placed sufficiently close to a compression corner, can prevent the separation of a supersonic flow due to an adverse pressure gradient.
2) The vortex generator energizes the low momentum fluid of the boundary layer by an expansion process around the generator body, in addition to the energizing action of the tip vortex and the streamwise vortex formed along the base of the generator. For this investigation the effects of the two mechanisms were not separable.
3) The region of effectiveness of the generator was limited to a very narrow region directly behind the generator trailing edge.

4) The performance of each generator was related more to chord length than to generator span.

5) Noticeable three-dimensional perturbations were found in the turbulent reattaching flow on the ramp in the absence of the generators.

REFERENCES

1. Wuerer, J. E., and F. I. Clayton, "Flow Separation in High Speed Flight, A Review of the State-of-the-Art," Douglas Report SM 46429, April 1965.

2. Kaufman, L. G., et al., "A Review of Hypersonic Flow Separation and Control Characteristics," United States Air Force, Aeronautical Systems Division, TDR-62-168, March 1962.

3. Gillette, W. B., "Separation Measurements of Supersonic Turbulent Boundary Layers Over Compression Corners," Defense Research Laboratory Report No. 543 (DRL-543, CR-26), Defense Research Laboratory, The University of Texas, Austin, Texas, July 1966.

4. Pearcy, H. H., and C. M. Stuart, "Methods of Boundary Layer Control for Postponing and Alleviating Buffeting and Other Effects of Shock-Induced Separation," AIAA Fairchild Fund Paper 22, June 1959.

5. Edwards, J. B. W., "Free Flight Tests of Vortex Generator Configurations at Transonic Speeds," R.A.E. Tech. Note-Aero. 2862, December 1962.

6. Whitten, J. W., "The Drag of Vane-Type Vortex Generators in Compressible Turbulent Flow," Defense Research Laboratory Report No. 556 (DRL-556), Defense Research Laboratory, The University of Texas, Austin, Texas, August 1967.

7. "Equations, Tables and Charts for Compressible Flow," NACA Report 1135, U. S. Government Printing Office, Washington, D. C., 1953.

8. Sterrett, J. R., and J. C. Emery, "Experimental Separation Studies for Two-Dimensional Wedges and Curved Surfaces at Mach Numbers of 4.8 to 6.2," NASA TN-D-1014, February 1962.

9. Kaufman, L. G., et al., "An Investigation of Hypersonic Flow Separation and Control Characteristics," United States Air Force, Research and Technology Division, AFFDL-TR-64-174, January 1965.

10. Ginoux, J. J., "The Existence of Three-Dimensional Perturbations in in the Reattachment of a Two-Dimensional Supersonic Boundary Layer after Separation," AGARD Report 272, 1960.

REFERENCES (Cont'd)

11. Roshko, A., and G. J. Thomke, "Observations of Turbulent Reattachment Behind an Axisymmetric Downstream-Facing Step in Supersonic Flow," AIAA Journal 4(6), June 1966.

12. McCabe, A., "The Three-Dimensional Interaction of a Shock Wave with a Turbulent Boundary Layer," The Aeronautical Quarterly, Vol. XVII (3) August 1966.

TABLE I

VORTEX GENERATOR DIMENSIONS

Generator Number	b, in.	c, in.	R
1	0.50	1.00	0.50
2	0.25	1.00	0.25
3	0.25	0.50	0.50
4	0.50	0.50	1.00

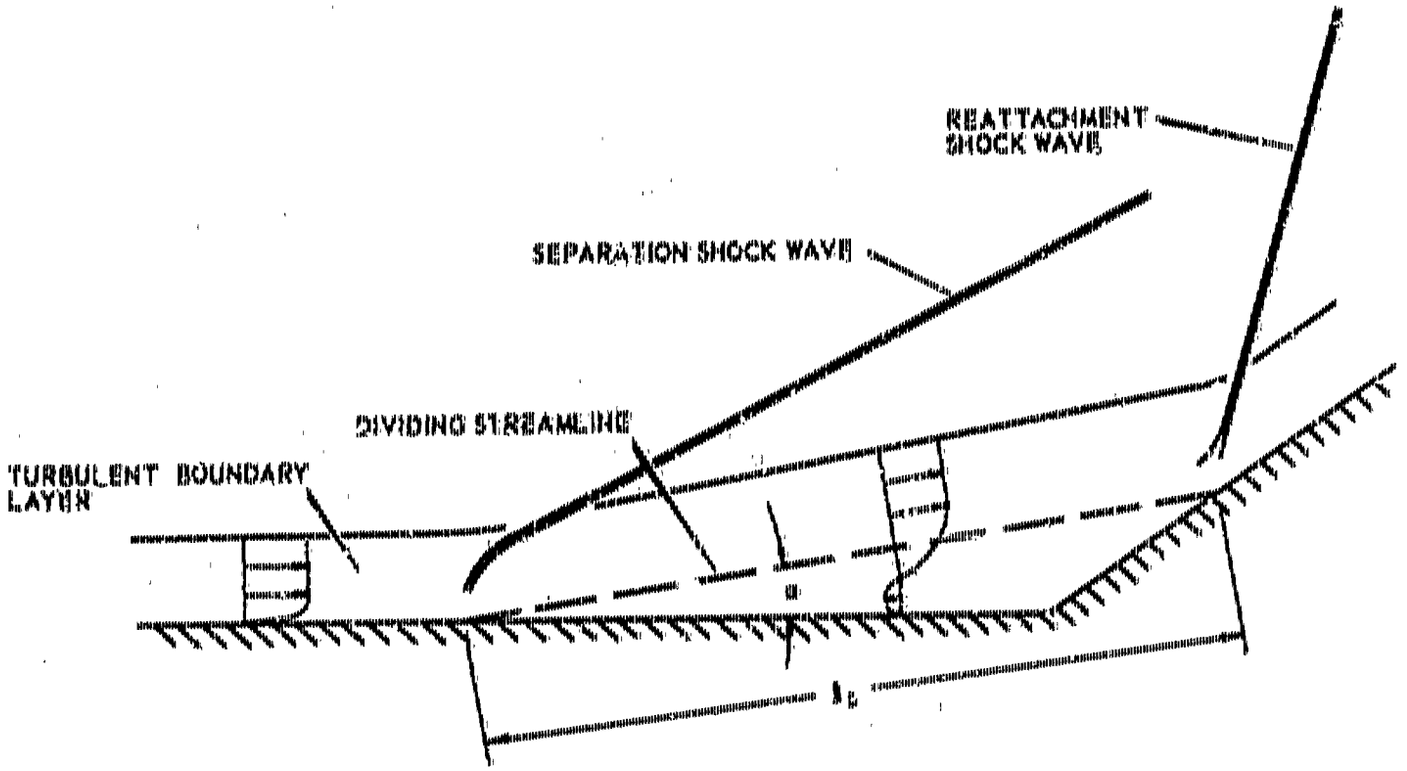

FIGURE 1
SEPARATION GEOMETRY FOR A COMPRESSION CORNER

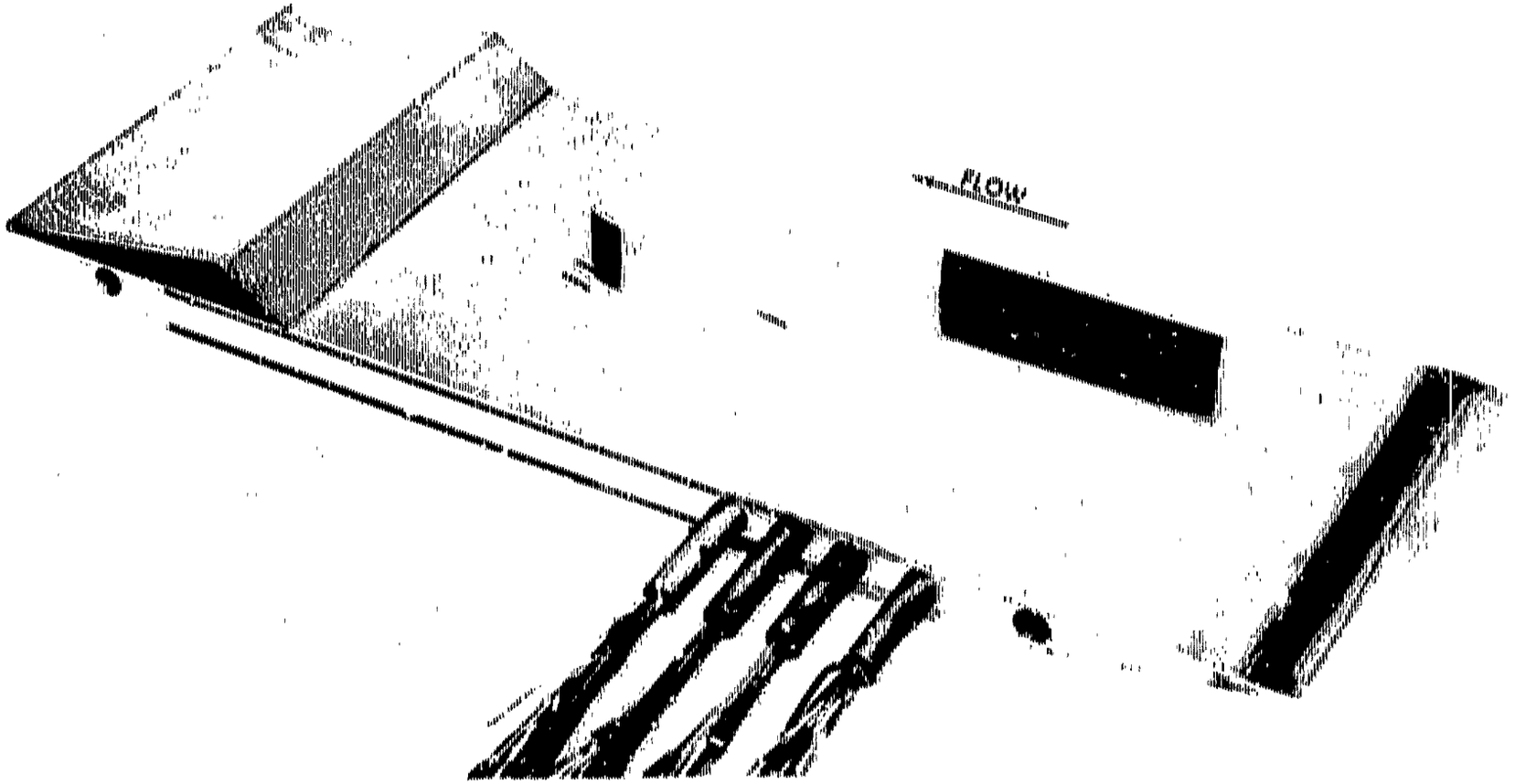

FIGURE 2
FLAT PLATE AND RAMP
WITH TYPICAL VORTEX GENERATORS

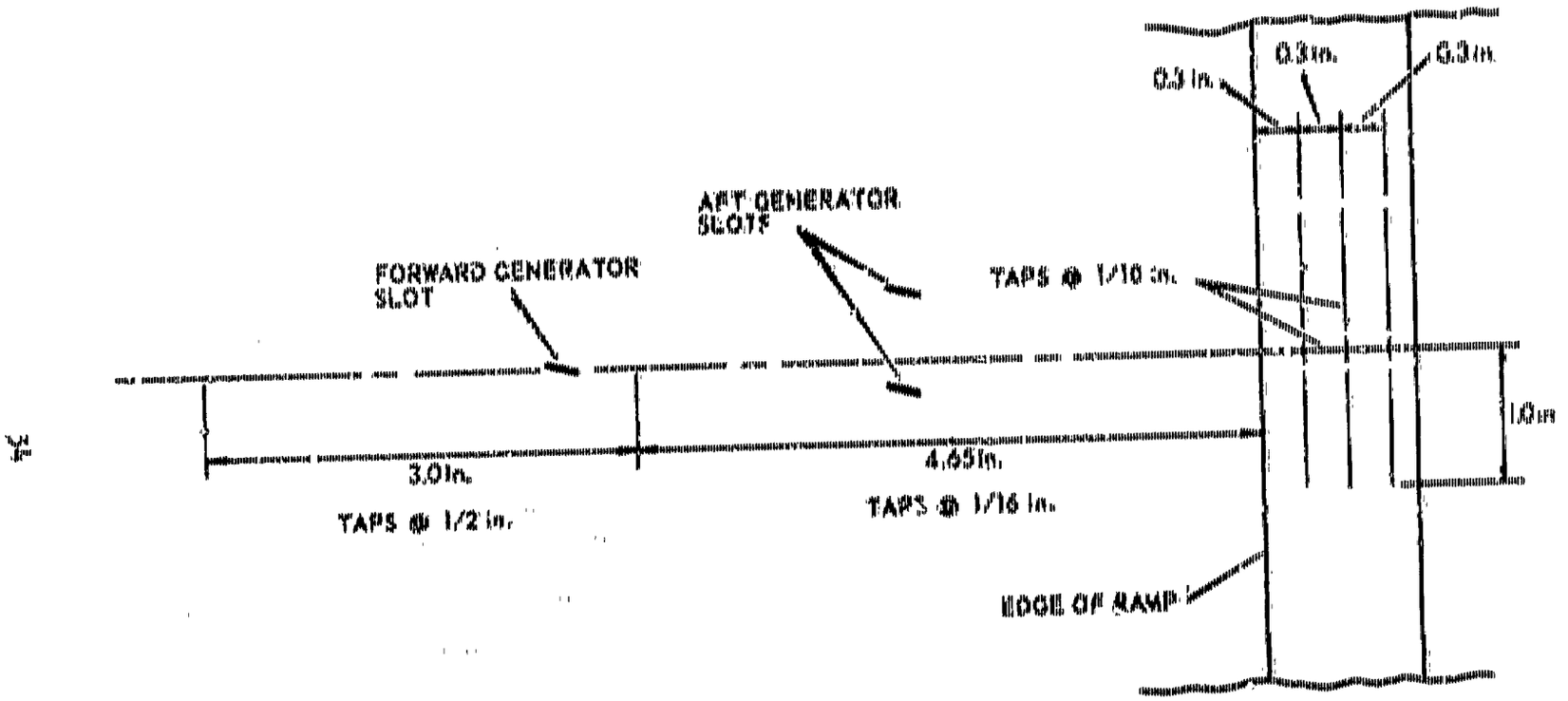

FIGURE 3
LOCATION OF PRESSURE TAPS ON
FLAT PLATE AND RAMP

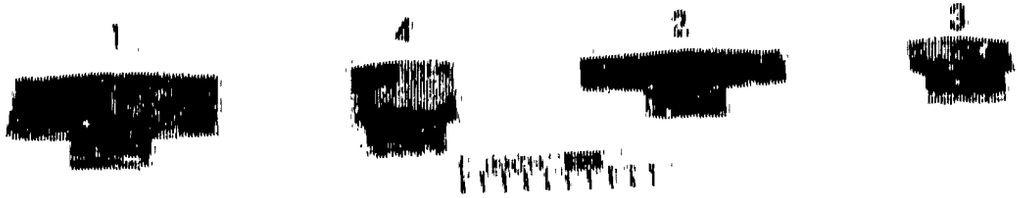

FIGURE 4
VORTEX GENERATORS

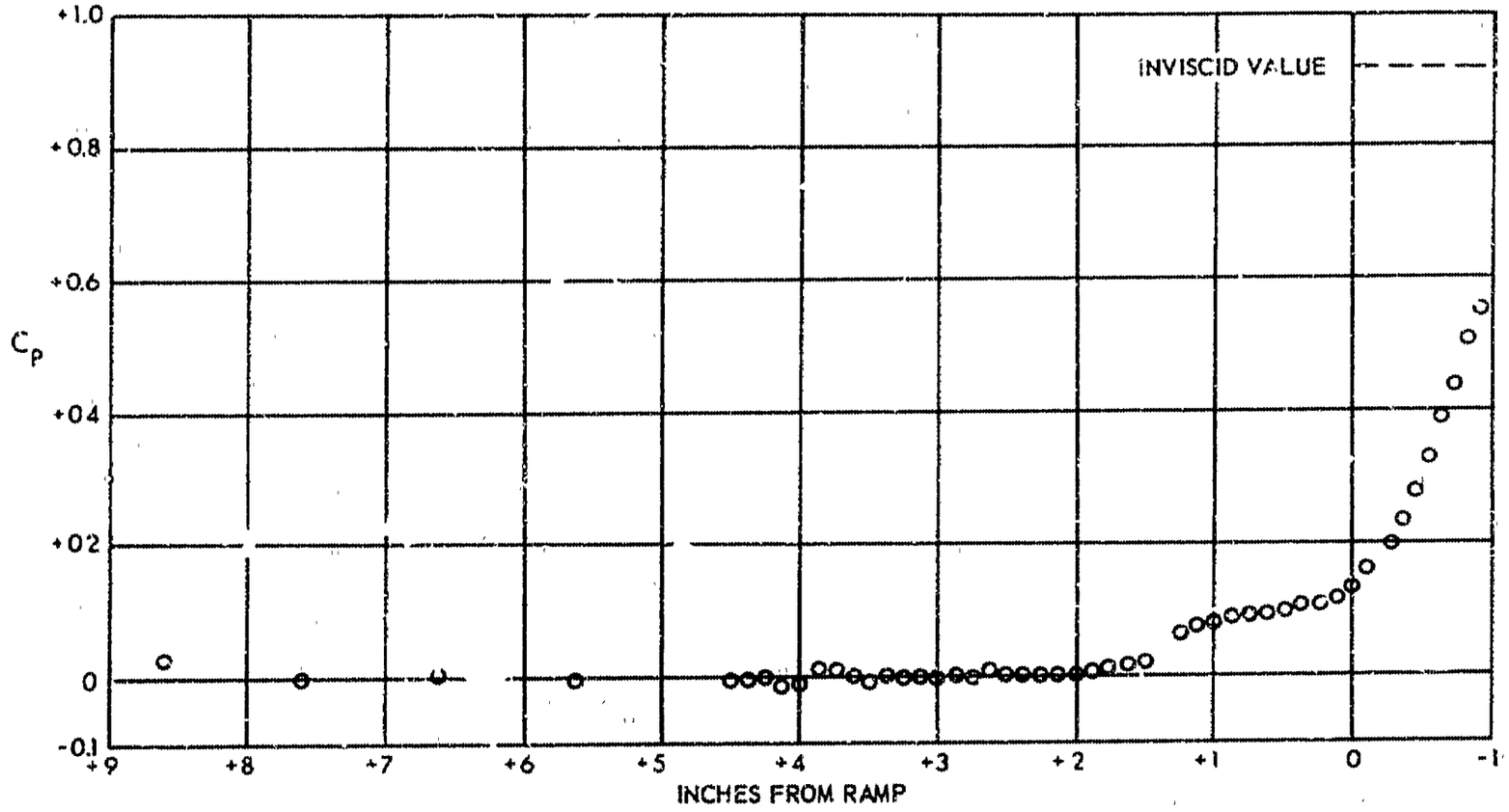

FIGURE 5a
CENTERLINE PRESSURE COEFFICIENTS FOR COMPRESSION CORNER

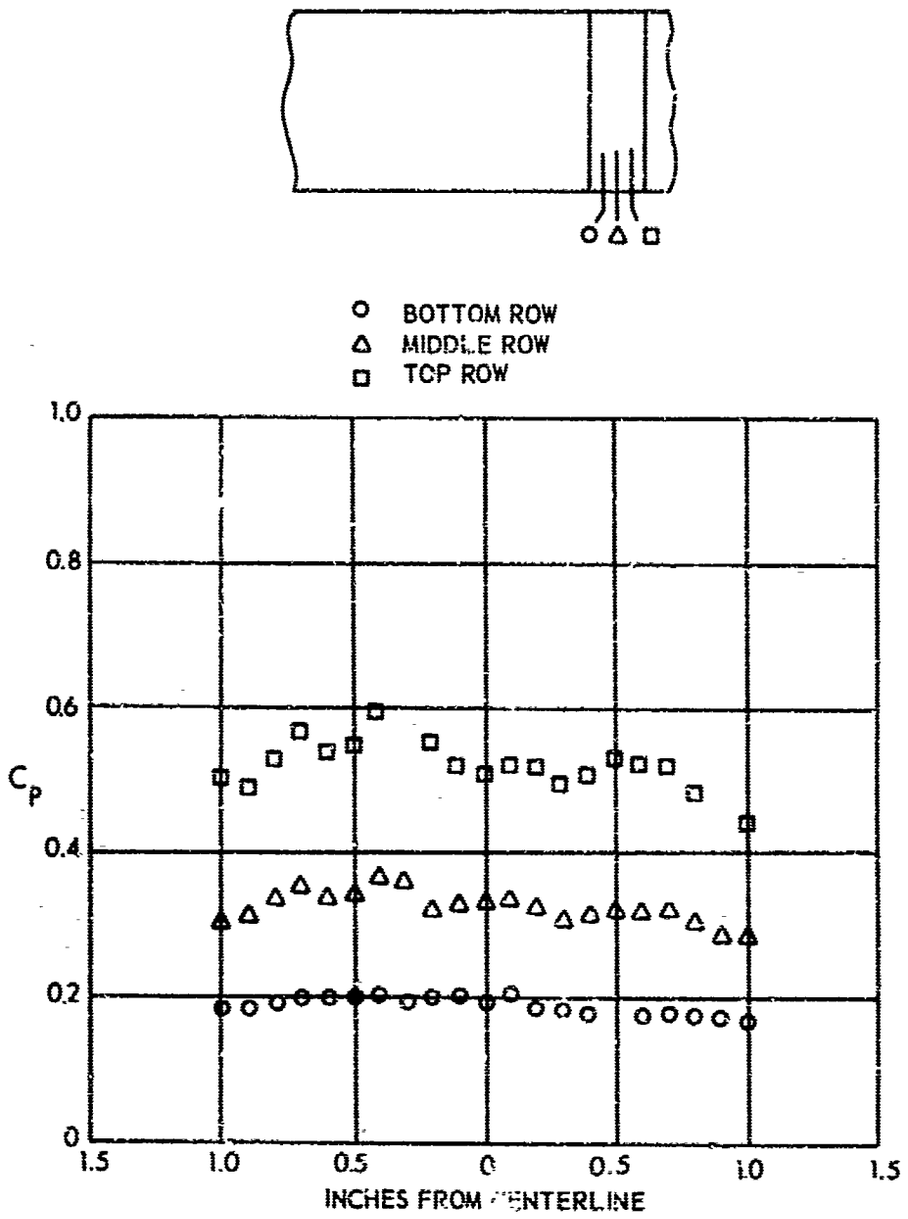

FIGURE 5b
SPANWISE PRESSURE COEFFICIENTS FOR COMPRESSION CORNER

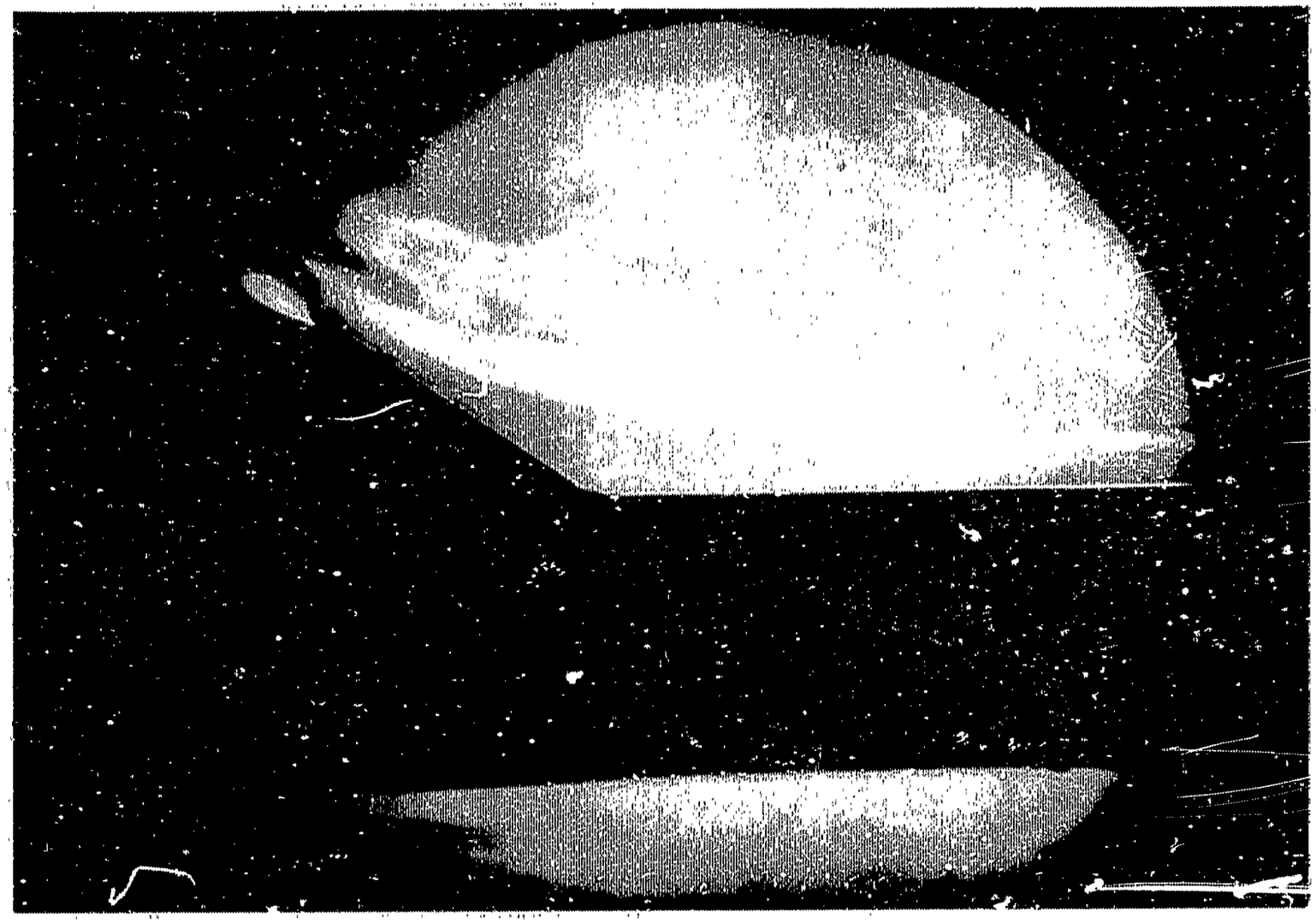

FIGURE 6
SCHLIEREN PHOTOGRAPH OF COMPRESSION CORNER

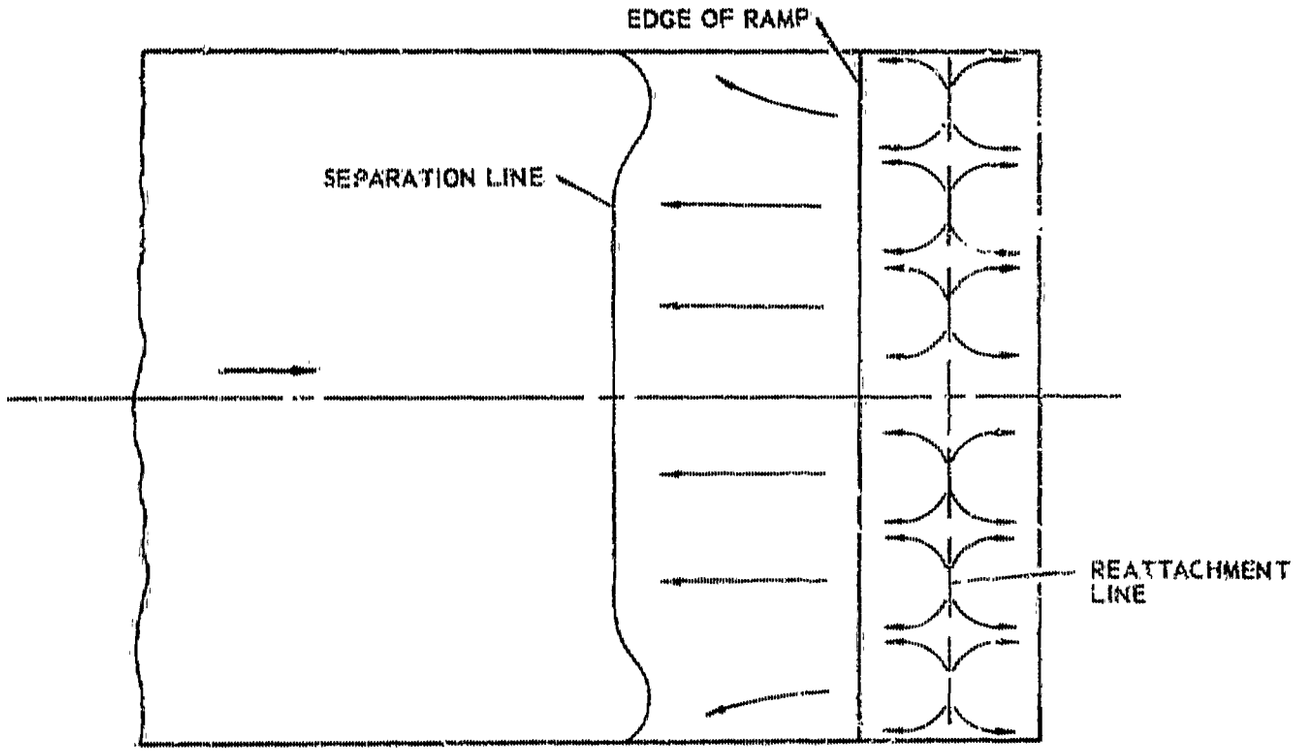

FIGURE 7
SKETCH OF TYPICAL OIL FLOW FOR SEPARATED FLOW

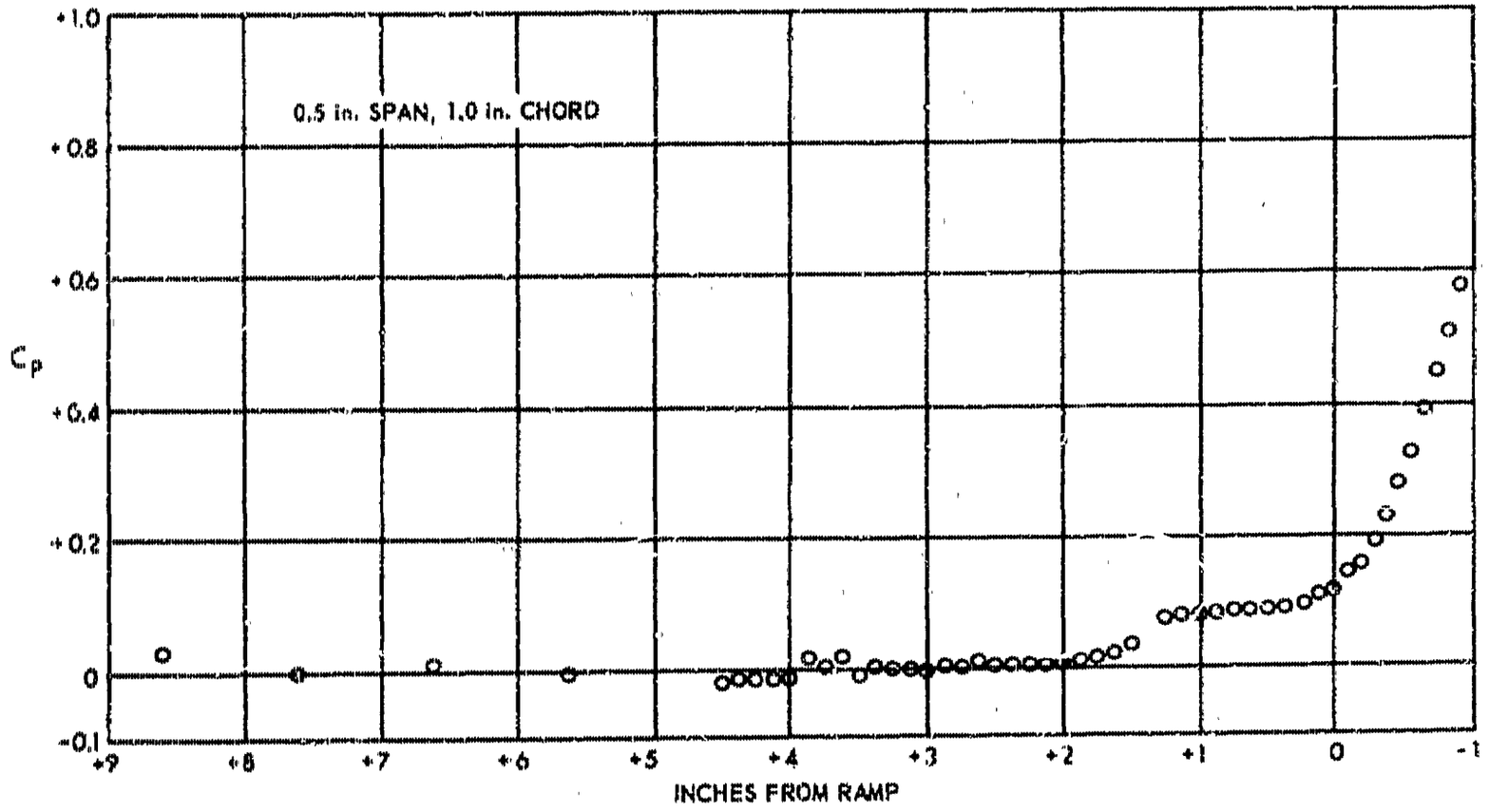

FIGURE 8a
CENTERLINE PRESSURE COEFFICIENTS FOR
GENERATOR No. 1 IN FORWARD POSITION

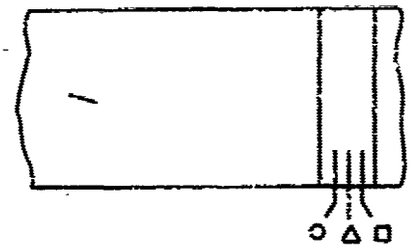

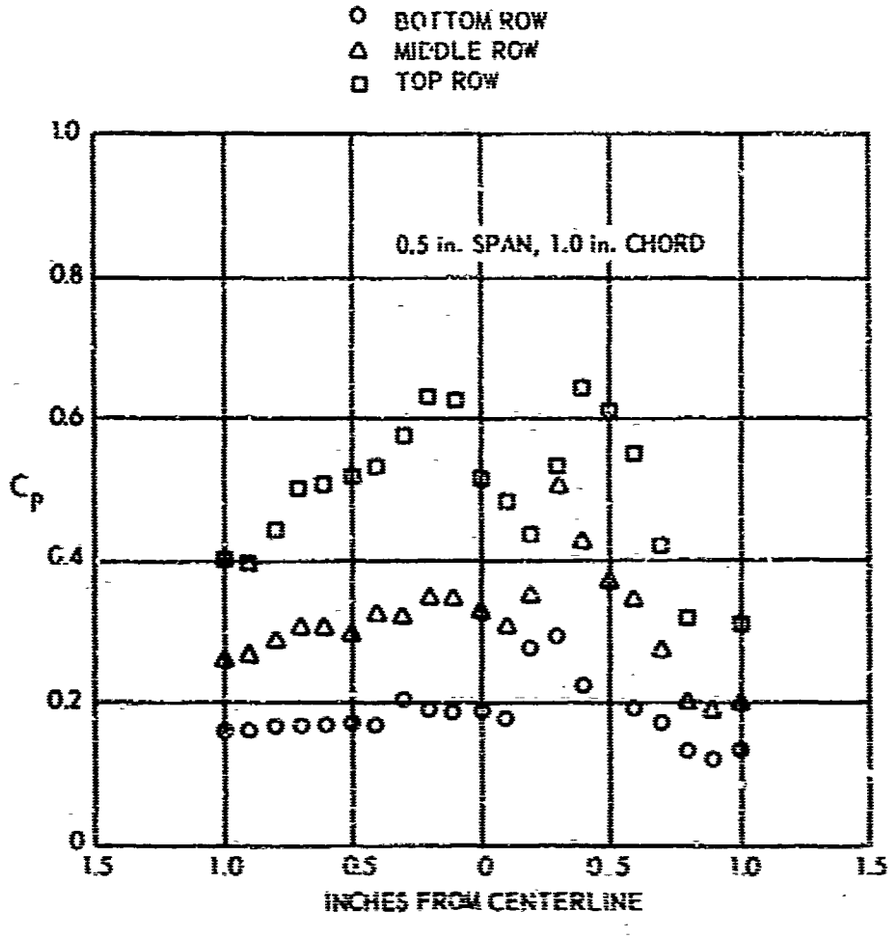

FIGURE 8b
SPANWISE PRESSURE COEFFICIENTS FOR
GENERATOR No. 1 IN FORWARD POSITION

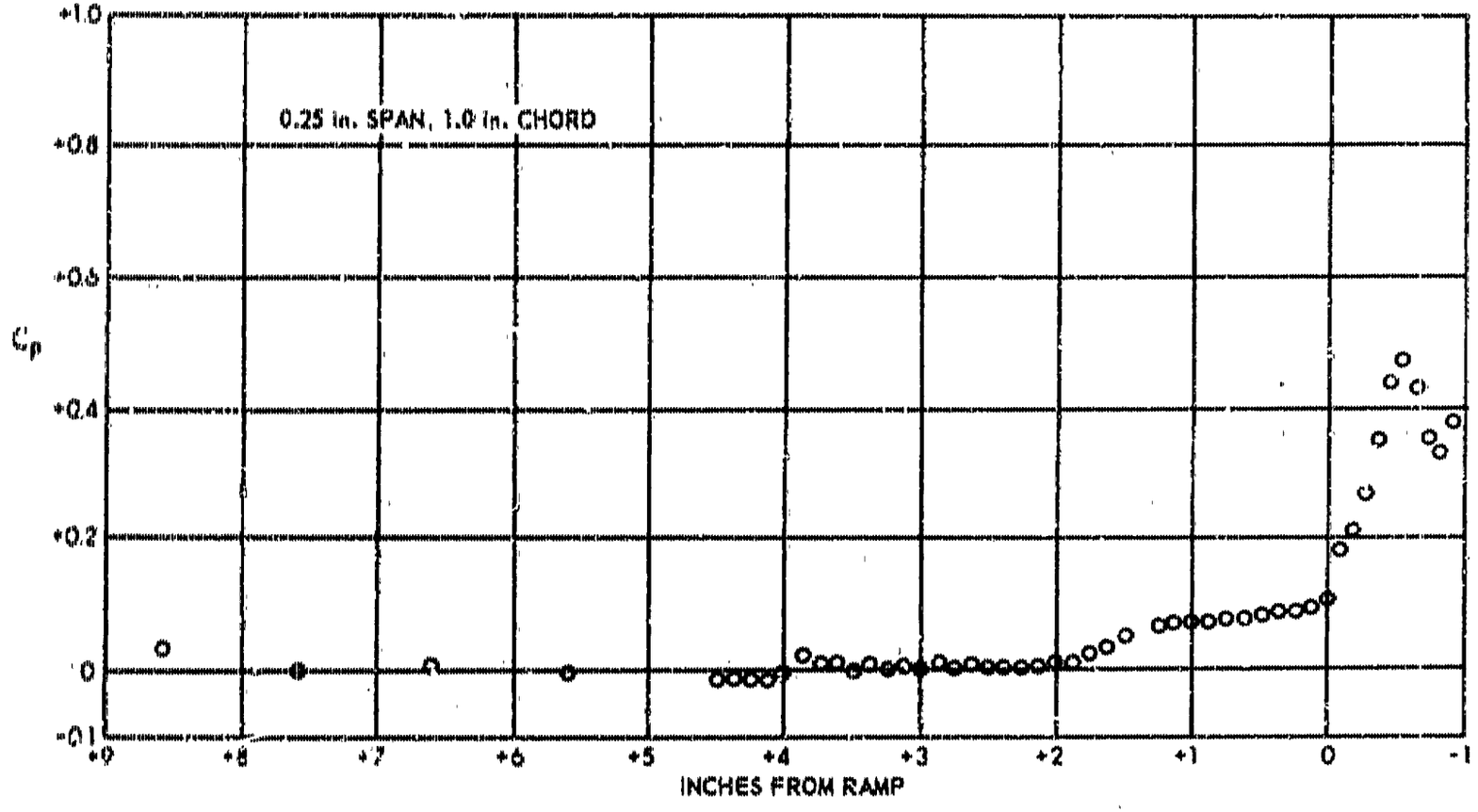

FIGURE 9a
CENTERLINE PRESSURE COEFFICIENTS FOR
GENERATOR No. 2 IN FORWARD POSITION

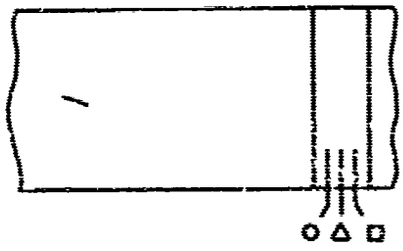

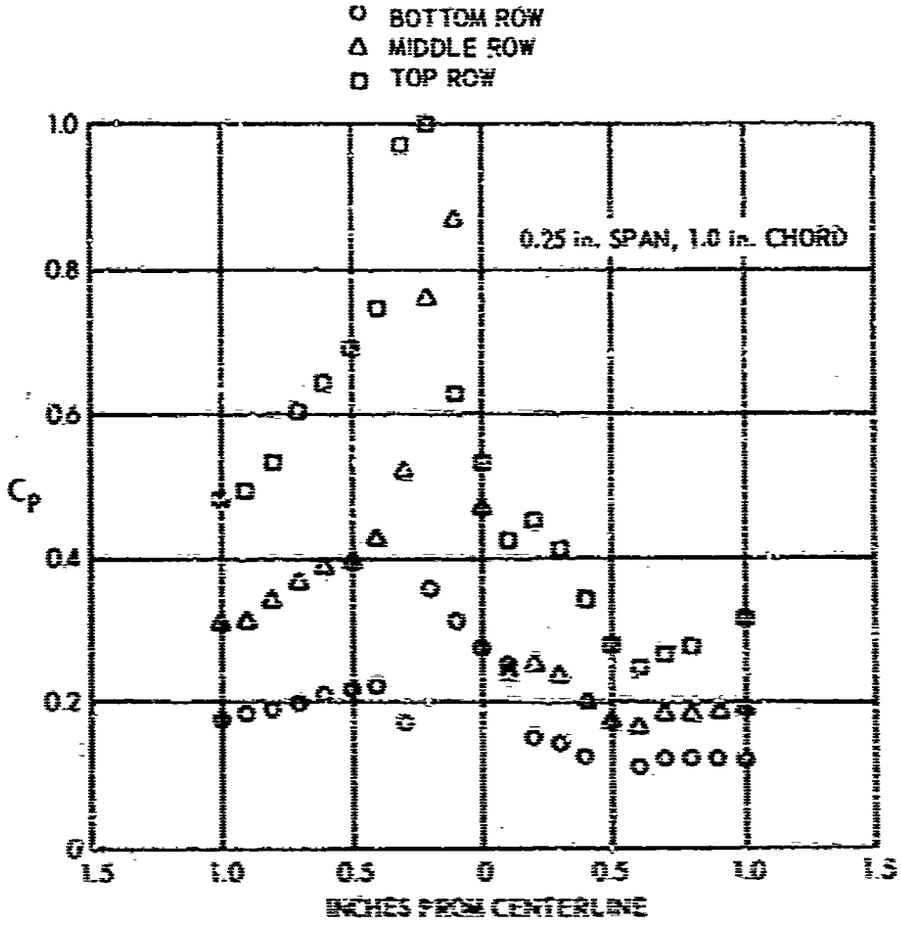

FIGURE 9a
SPANWISE PRESSURE COEFFICIENTS FOR
GENERATOR NO. 2 IN FORWARD POSITION

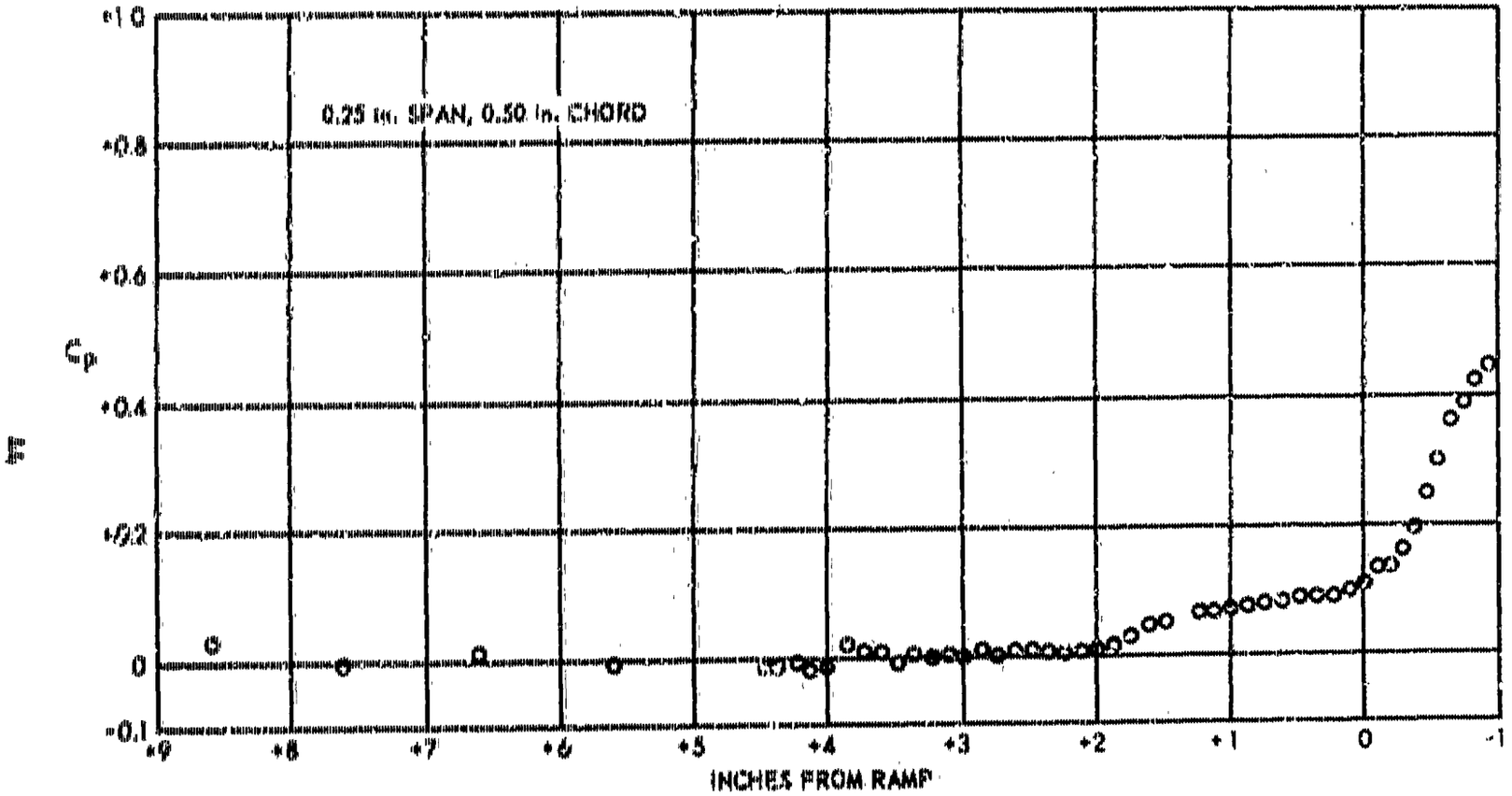

FIGURE 10a
CENTERLINE PRESSURE COEFFICIENTS FOR
GENERATOR No. 3 IN FORWARD POSITION

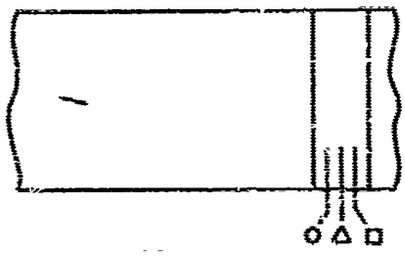

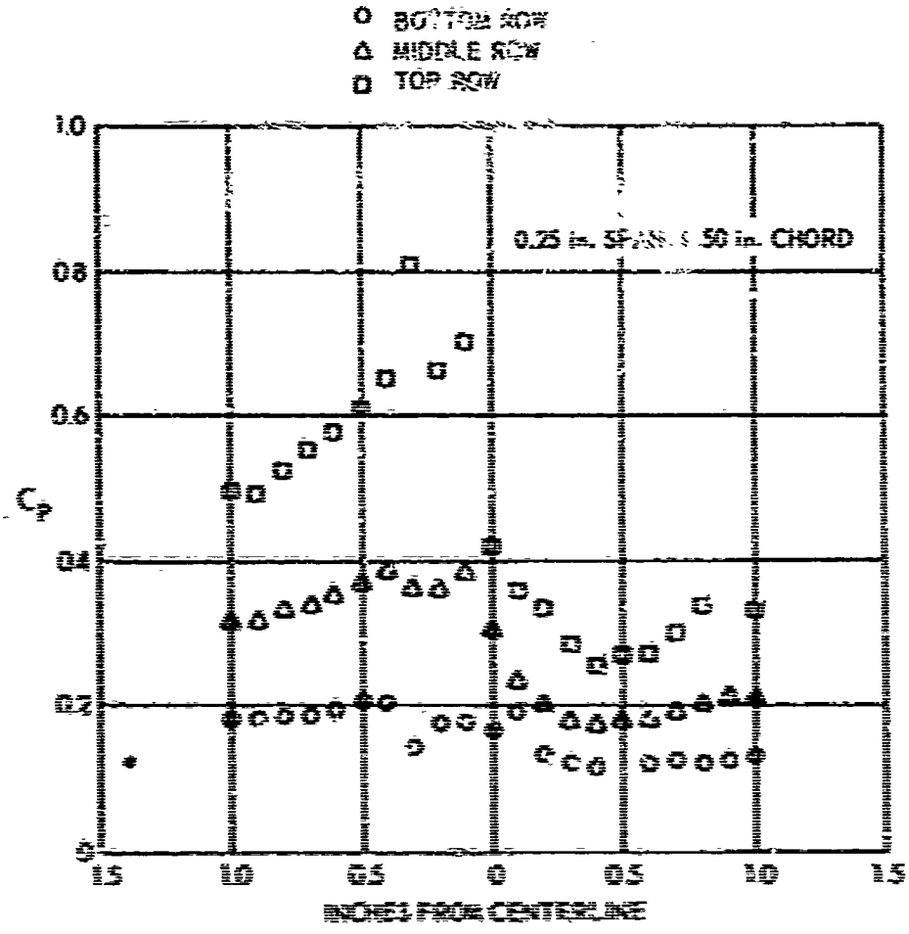

FIGURE 16b
SPANWISE PRESSURE COEFFICIENTS FOR
GENERATOR No. 3 IN FORWARD POSITION

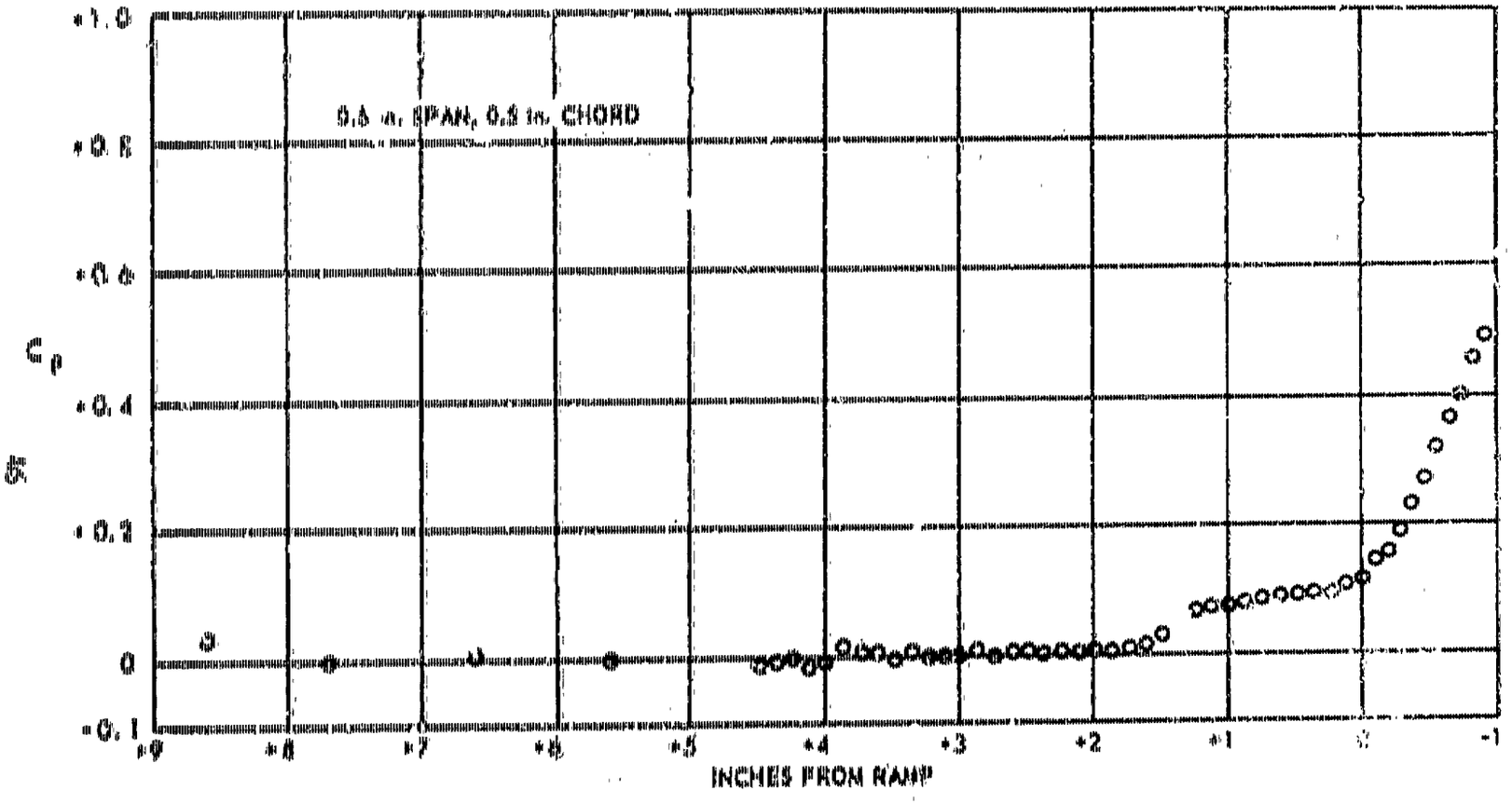

FIGURE 13a
CENTERLINE PRESSURE COEFFICIENTS FOR
GENERATOR No. 4 IN FORWARD POSITION

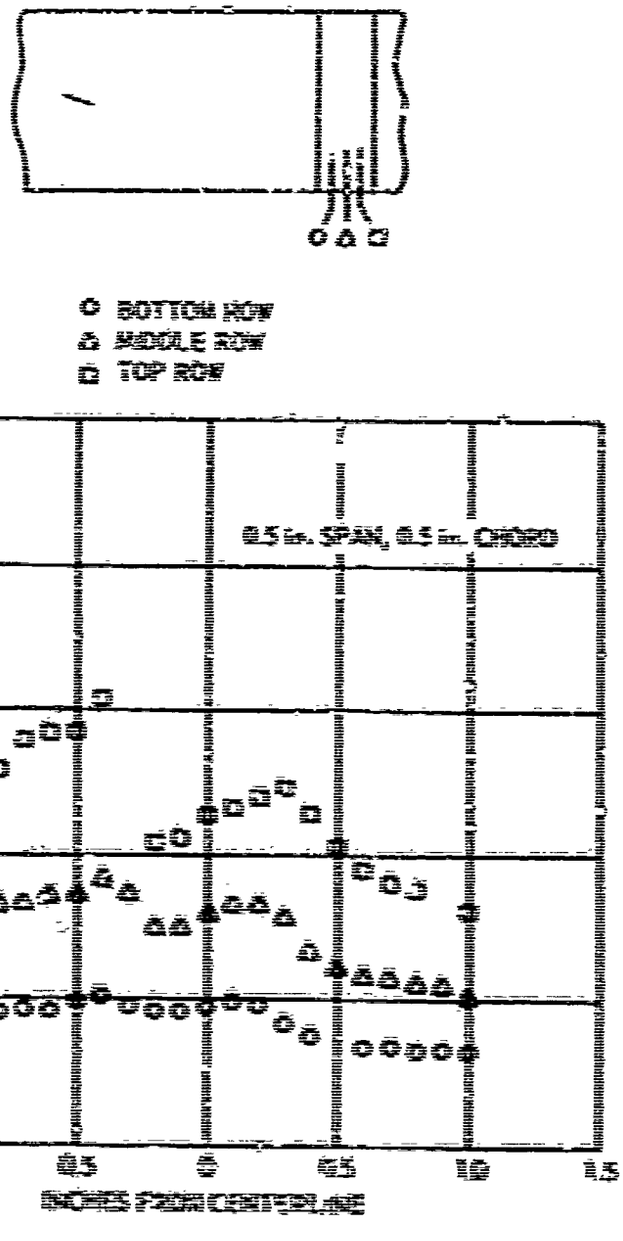

FIGURE 15.
SPANWISE PRESSURE COEFFICIENTS FOR
GENERATOR No. 4 IN FORWARD POSITION

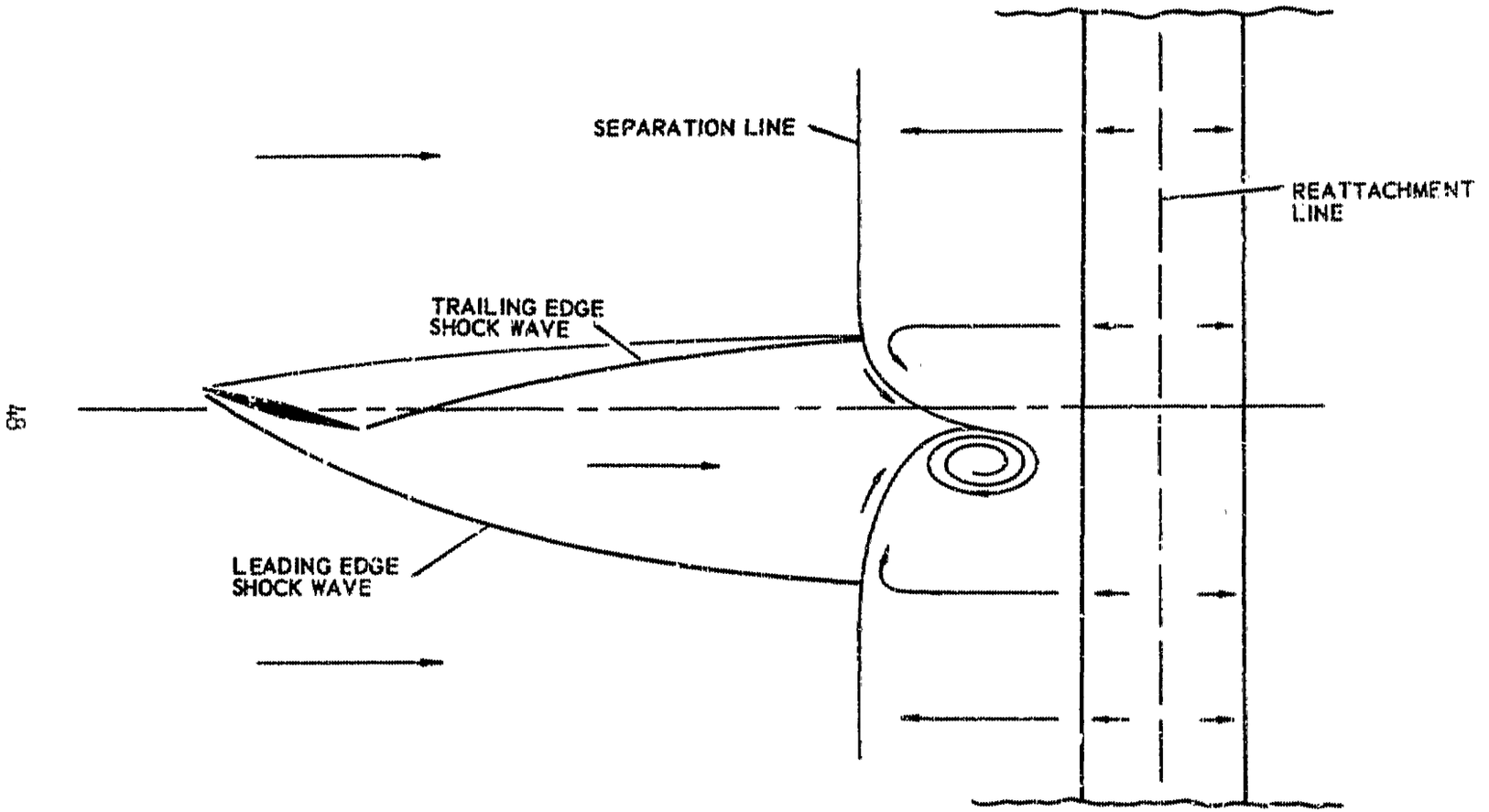

FIGURE 12
SKETCH OF OIL FLOW FOR
GENERATORS IN FORWARD POSITION

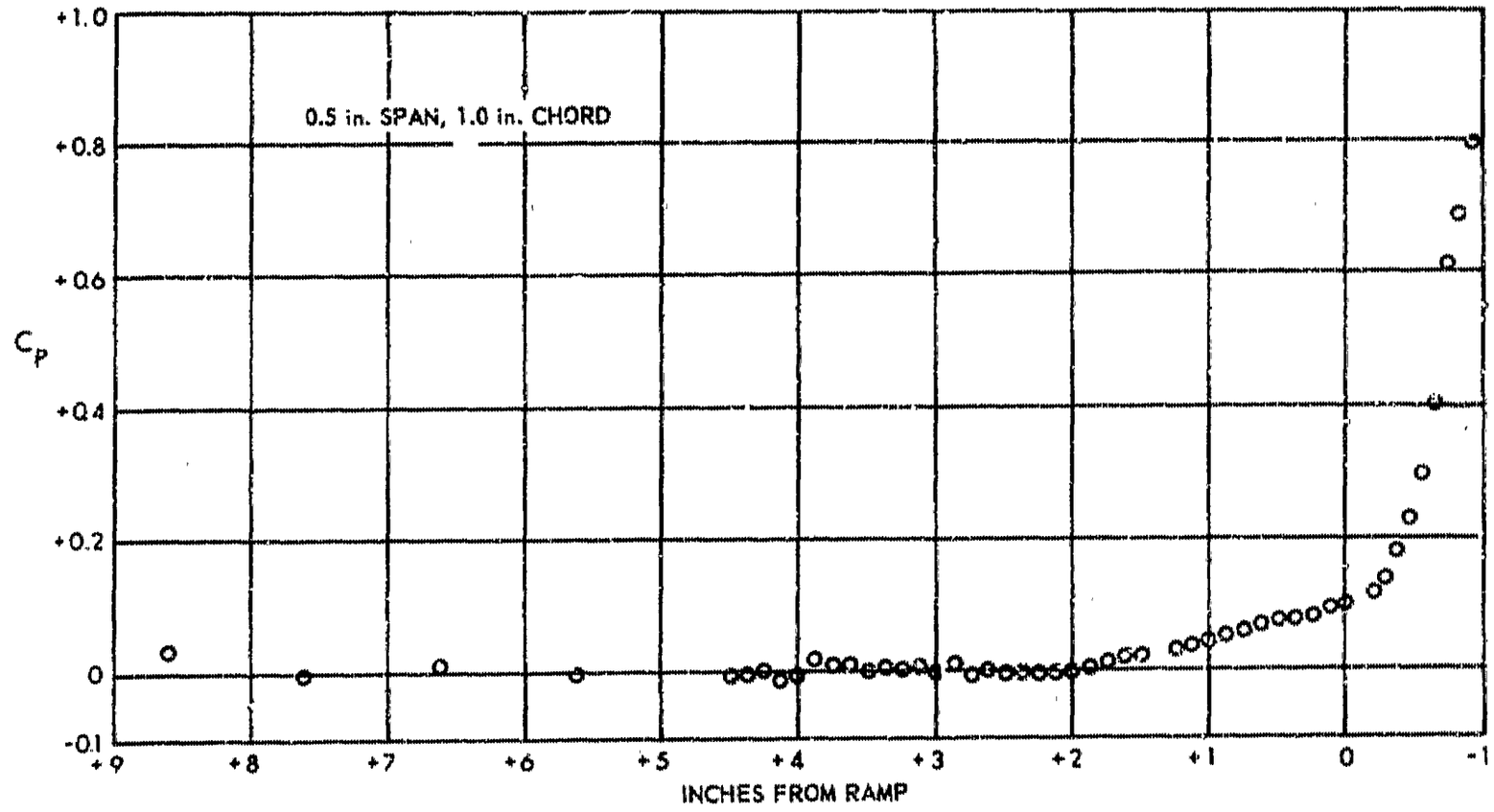

FIGURE 13a
CENTERLINE PRESSURE COEFFICIENTS FOR
GENERATOR No. 1 IN AFT RIGHT POSITION

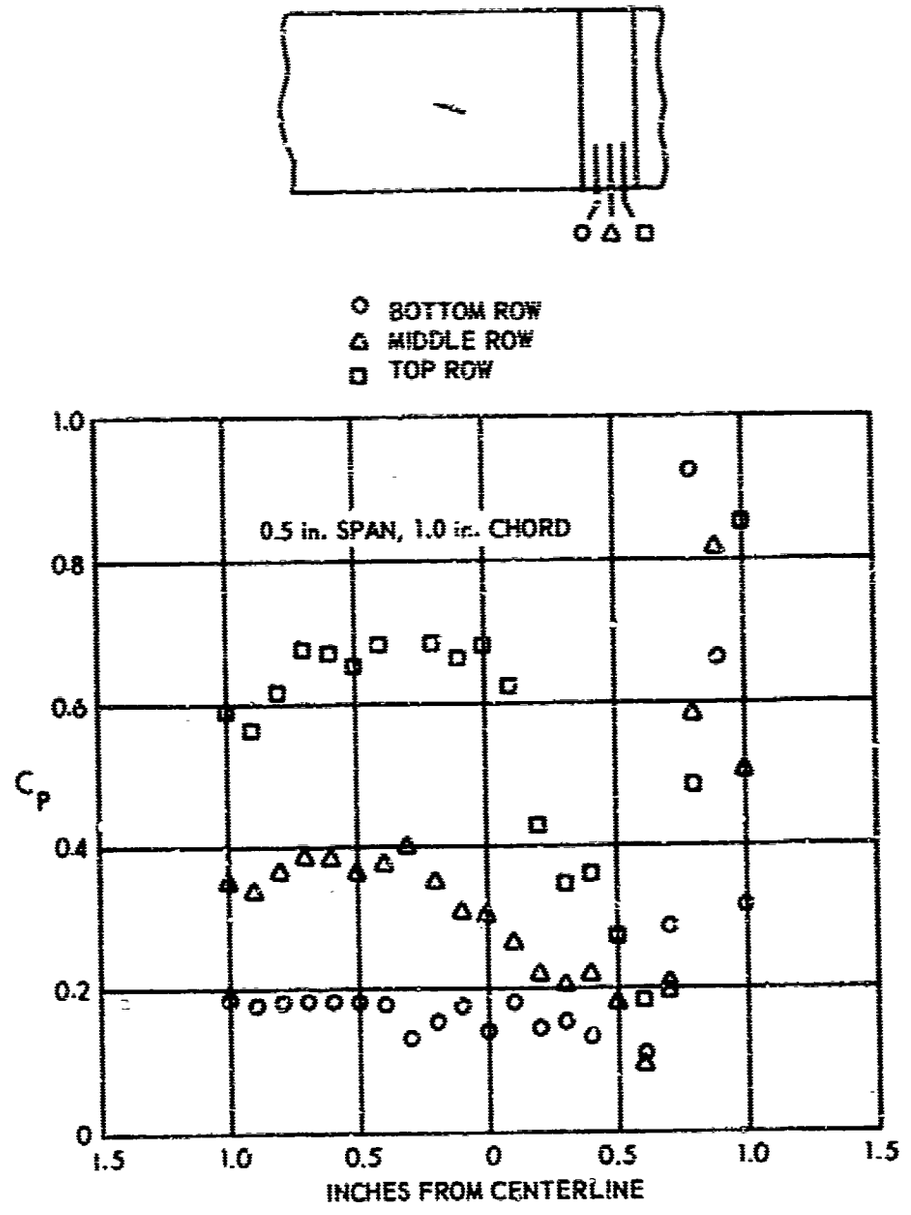

FIGURE 13b
SPANWISE PRESSURE COEFFICIENTS FOR
GENERATOR No. 1 IN AFT RIGHT POSITION

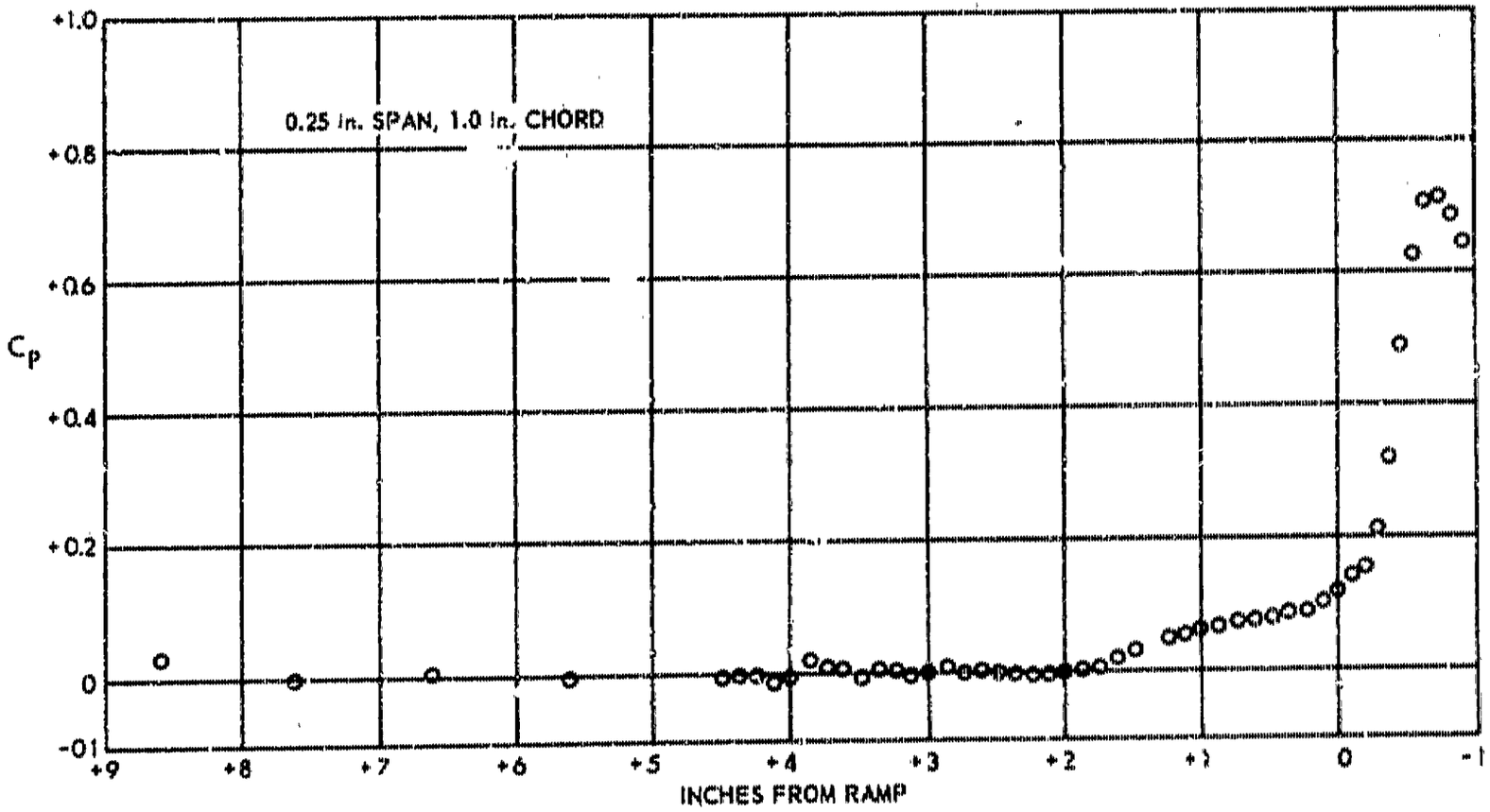

FIGURE 14a
CENTERLINE PRESSURE COEFFICIENTS FOR
GENERATOR No. 2 IN AFT RIGHT POSITION

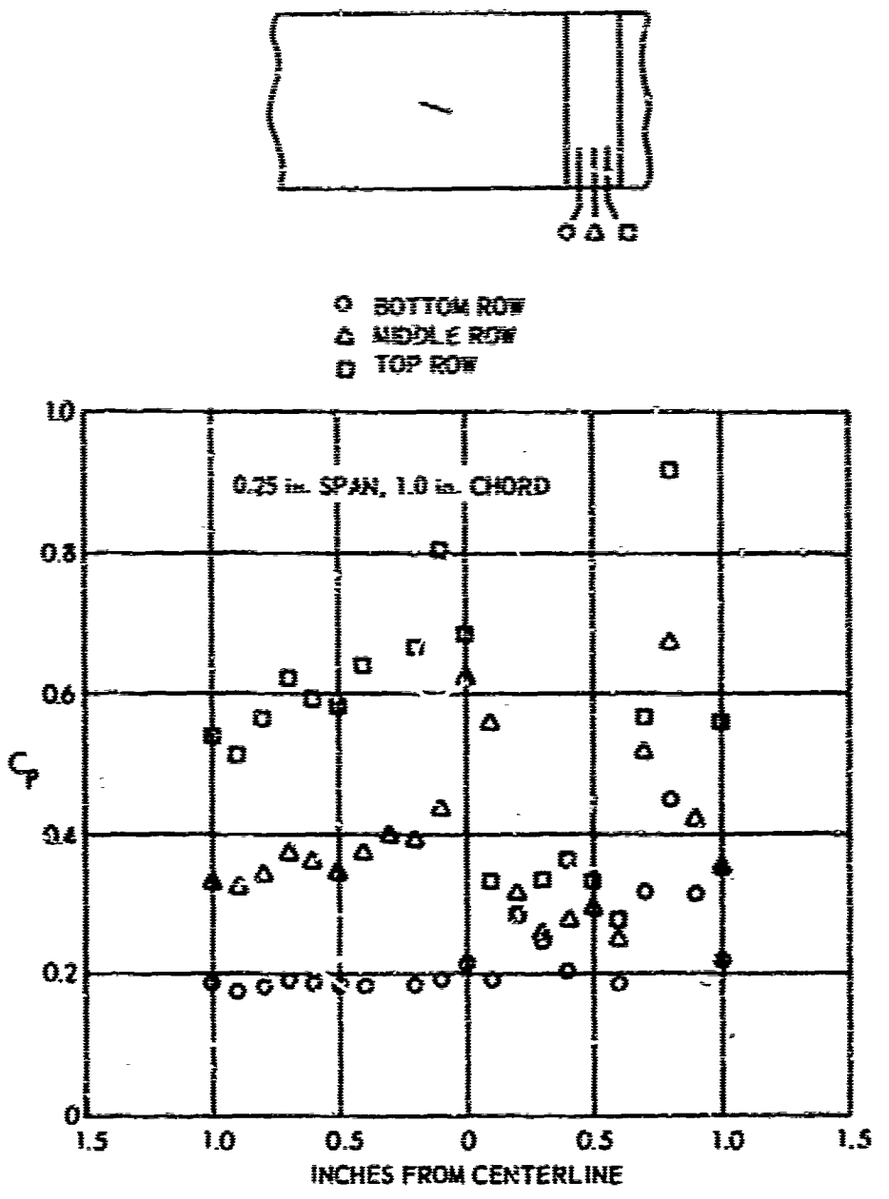

FIGURE 14b
SPANWISE PRESSURE COEFFICIENTS FOR
GENERATOR No. 2 IN AFT RIGHT POSITION

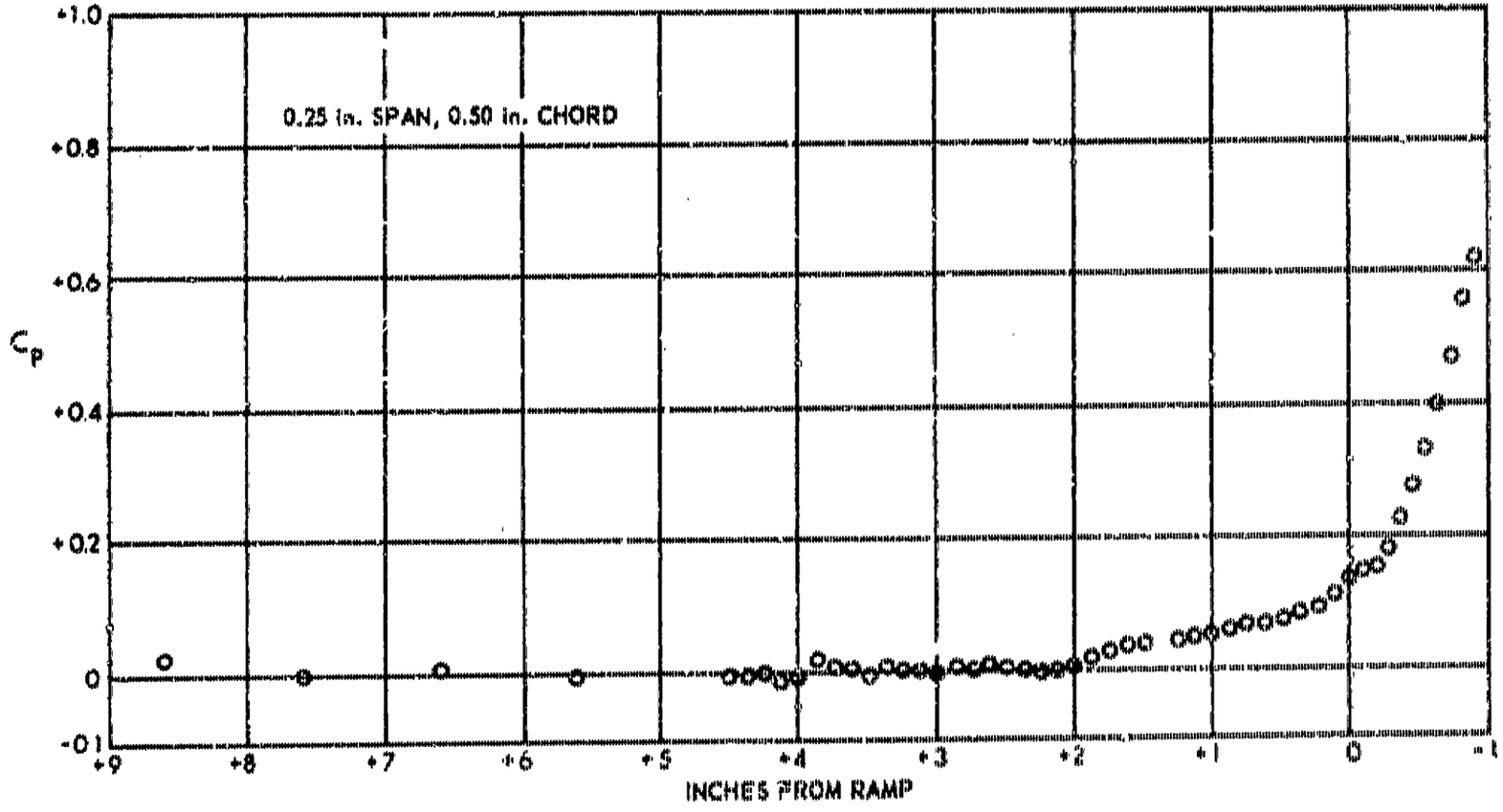

FIGURE 15a
CENTERLINE PRESSURE COEFFICIENTS FOR
GENERATOR No. 3 IN AFT RIGHT POSITION

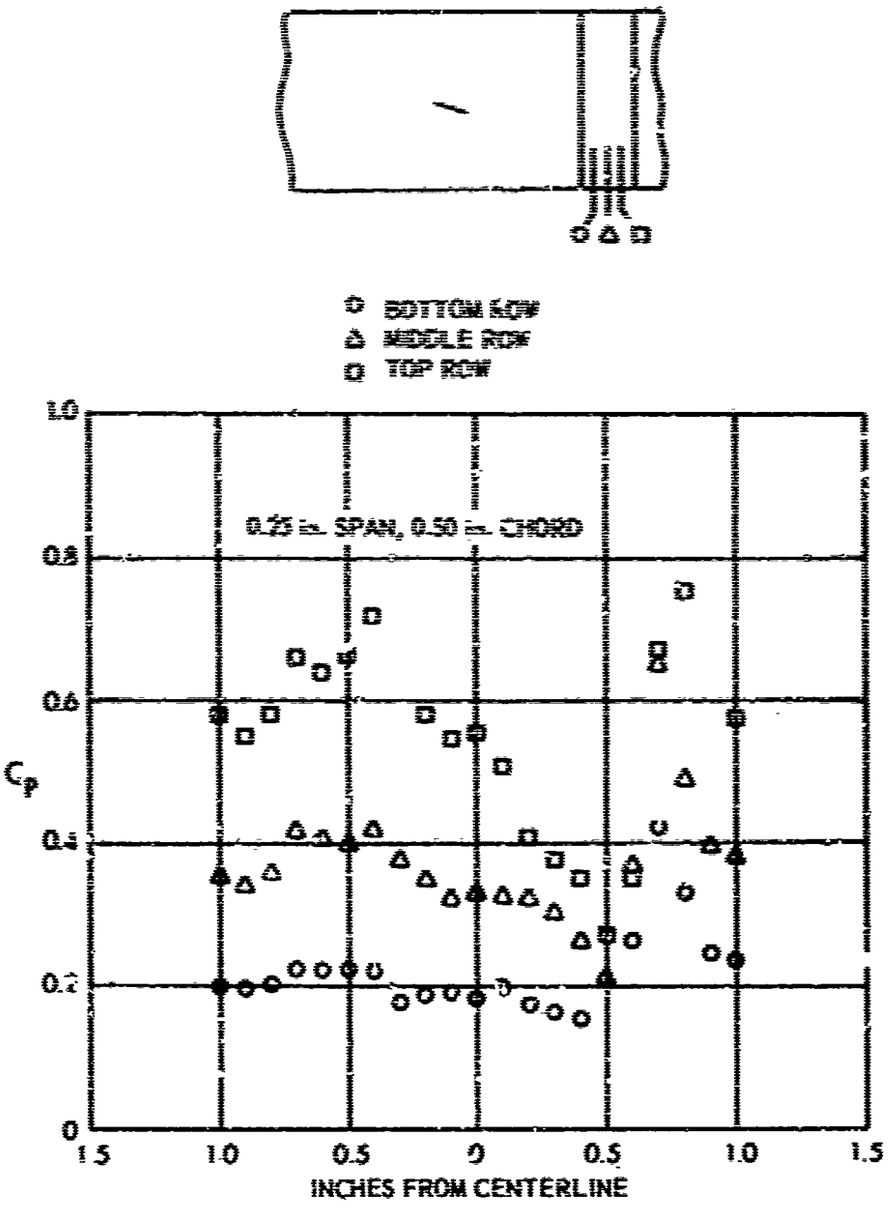

FIGURE 15b
SPANWISE PRESSURE COEFFICIENTS FOR
GENERATOR No. 3 IN AFT RIGHT POSITION

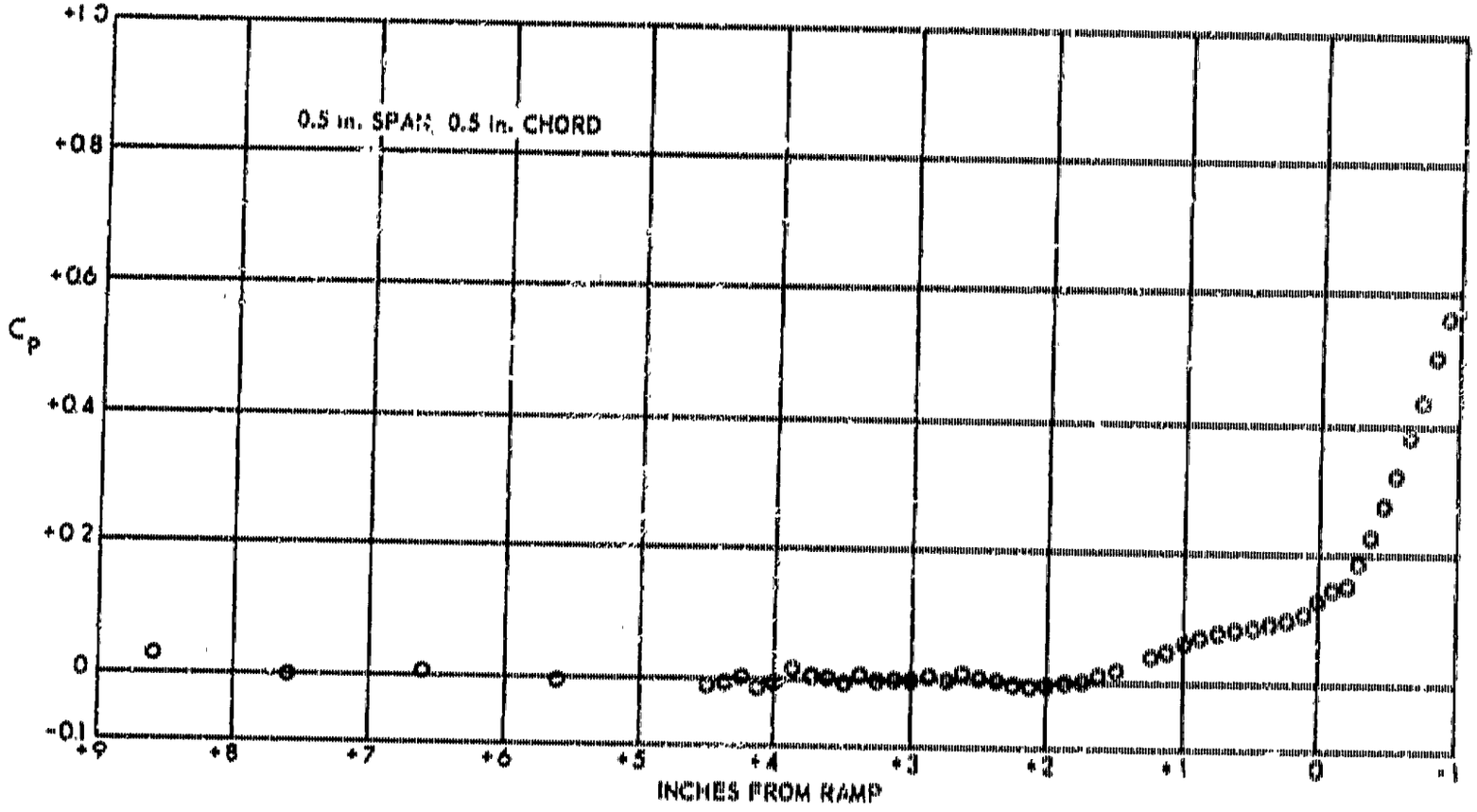

FIGURE 16a
CENTERLINE PRESSURE COEFFICIENTS FOR
GENERATOR No. 4 IN AFT RIGHT POSITION

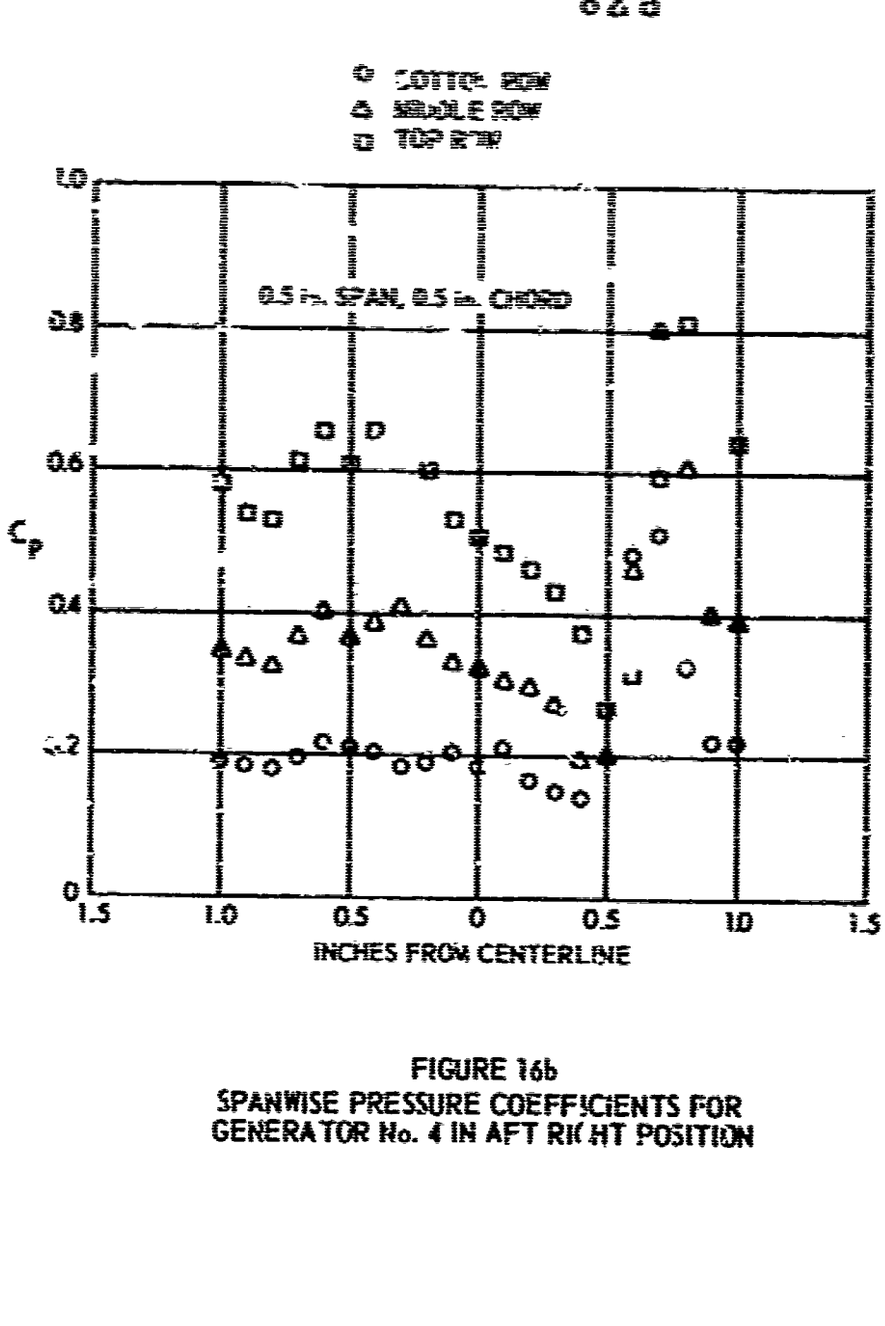

FIGURE 16b
SPANWISE PRESSURE COEFFICIENTS FOR
GENERATOR No. 4 IN AFT RIGHT POSITION

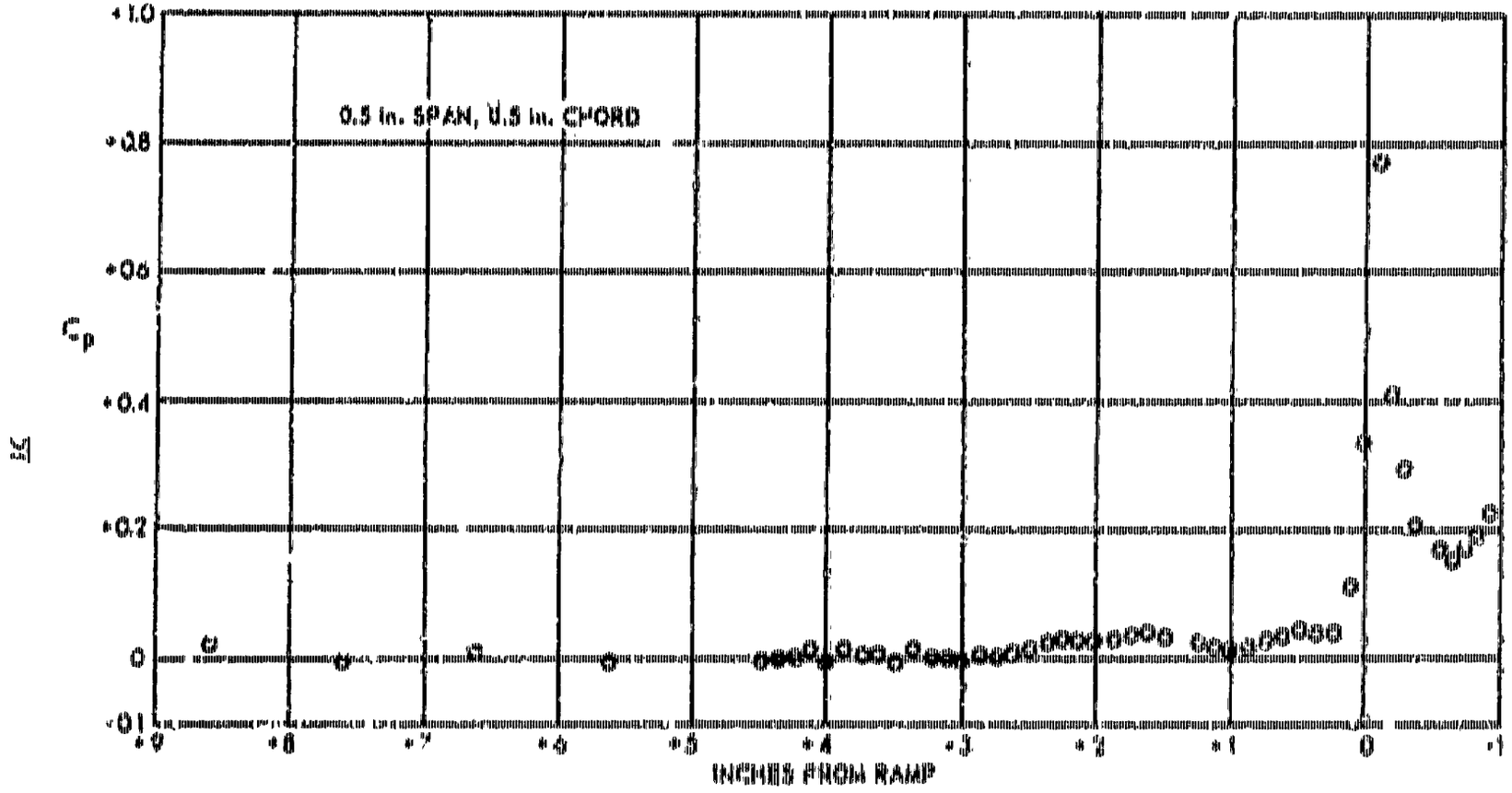

FIGURE 12a
CENTERLINE PRESSURE COEFFICIENTS FOR
GENERATOR No. 1 IN AFT LEFT POSITION

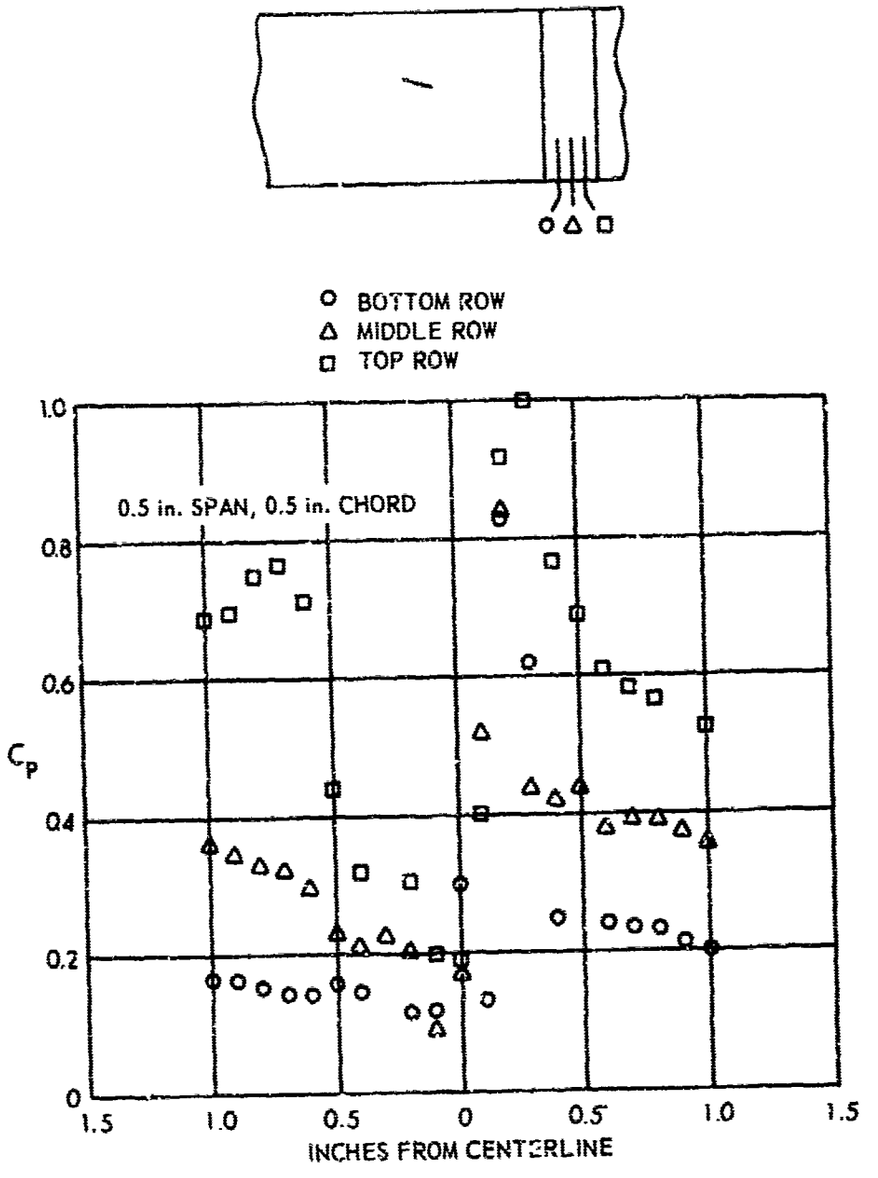

FIGURE 17b
SPANWISE PRESSURE COEFFICIENTS FOR
GENERATOR No. 1 IN AFT LEFT POSITION

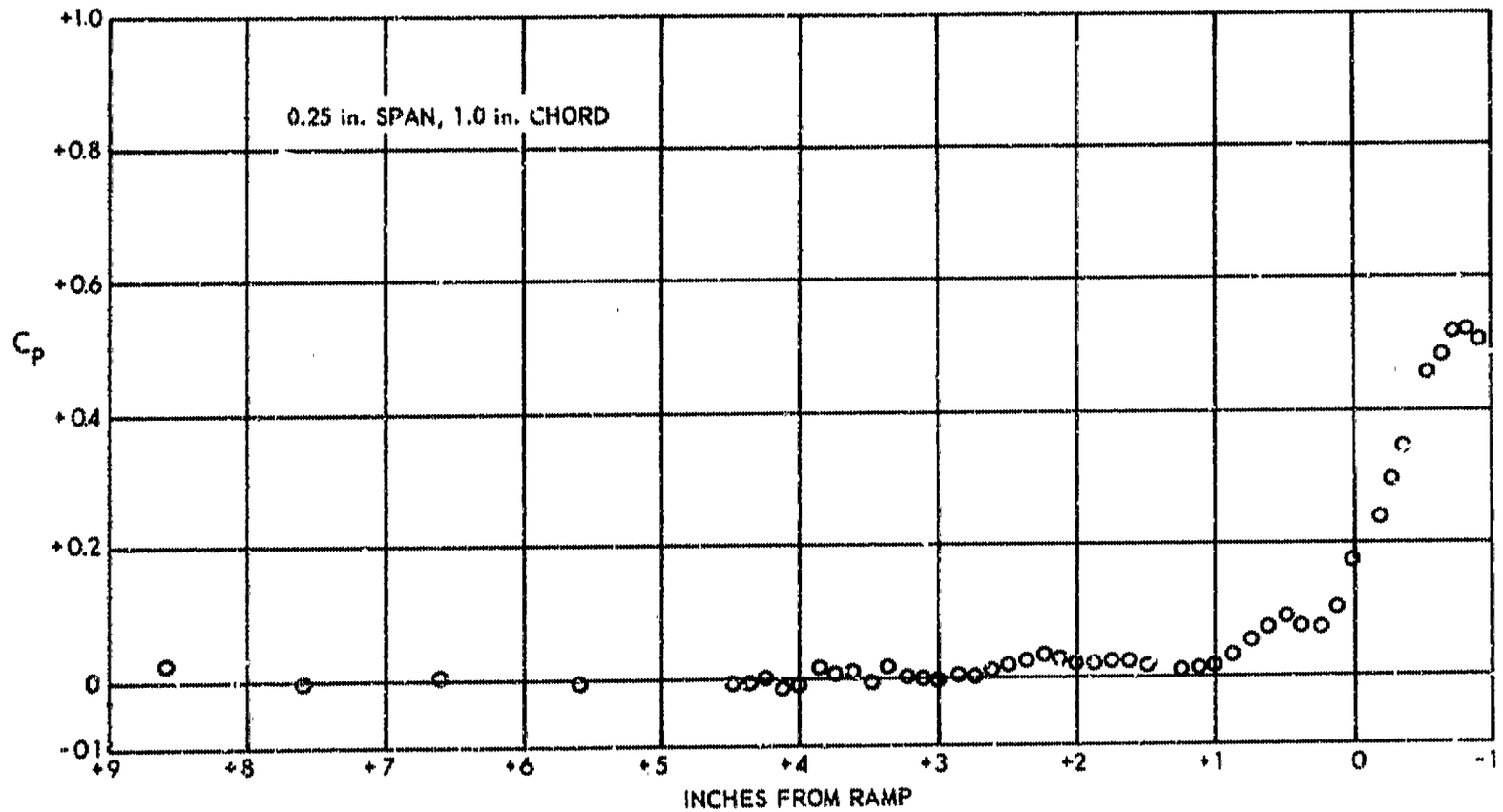

FIGURE 18a
CENTERLINE PRESSURE COEFFICIENTS FOR
GENERATOR No. 2 IN AFT LEFT POSITION

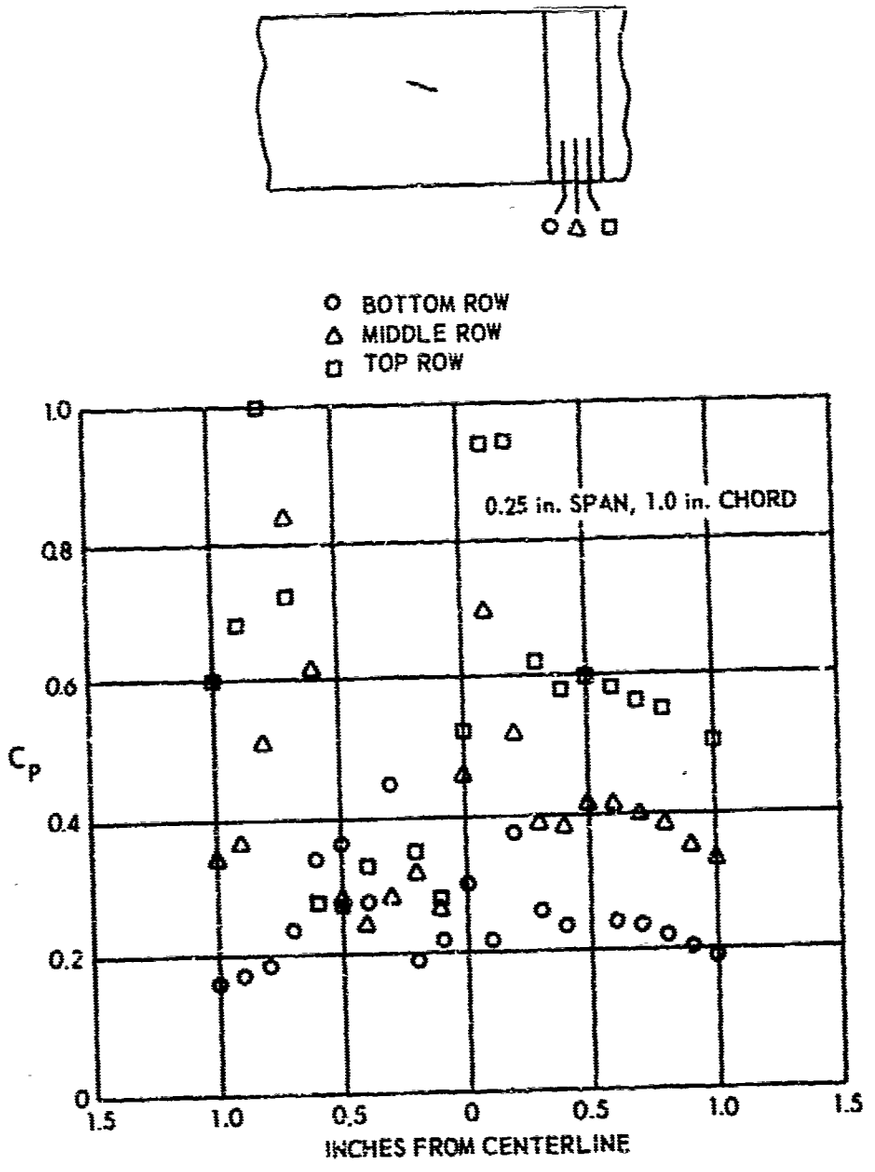

FIGURE 18b
SPANWISE PRESSURE COEFFICIENTS FOR
GENERATOR No. 2 IN AFT LEFT POSITION

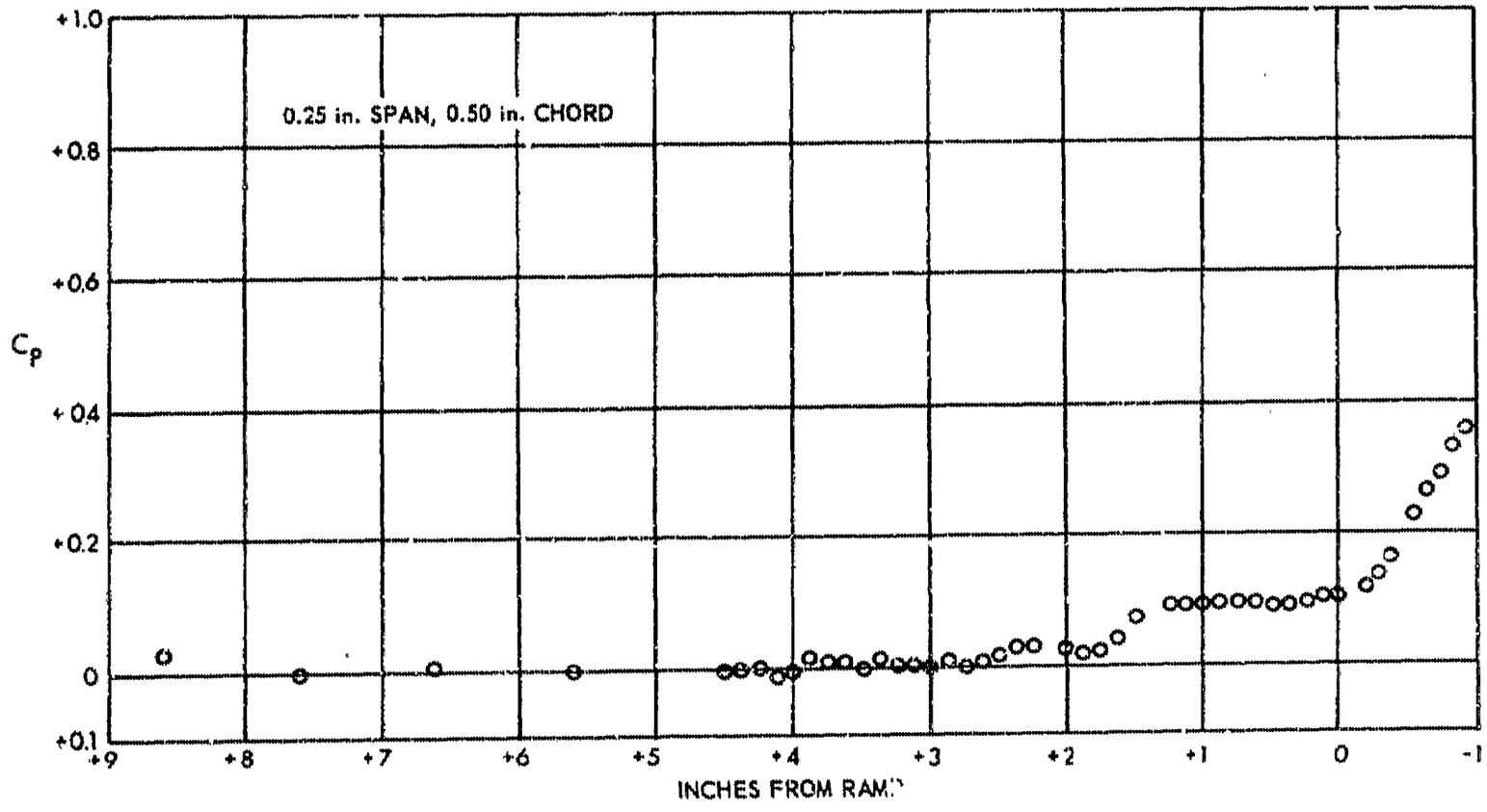

FIGURE 19a
CENTERLINE PRESSURE COEFFICIENTS FOR
GENERATOR No. 3 IN AFT LEFT POSITION

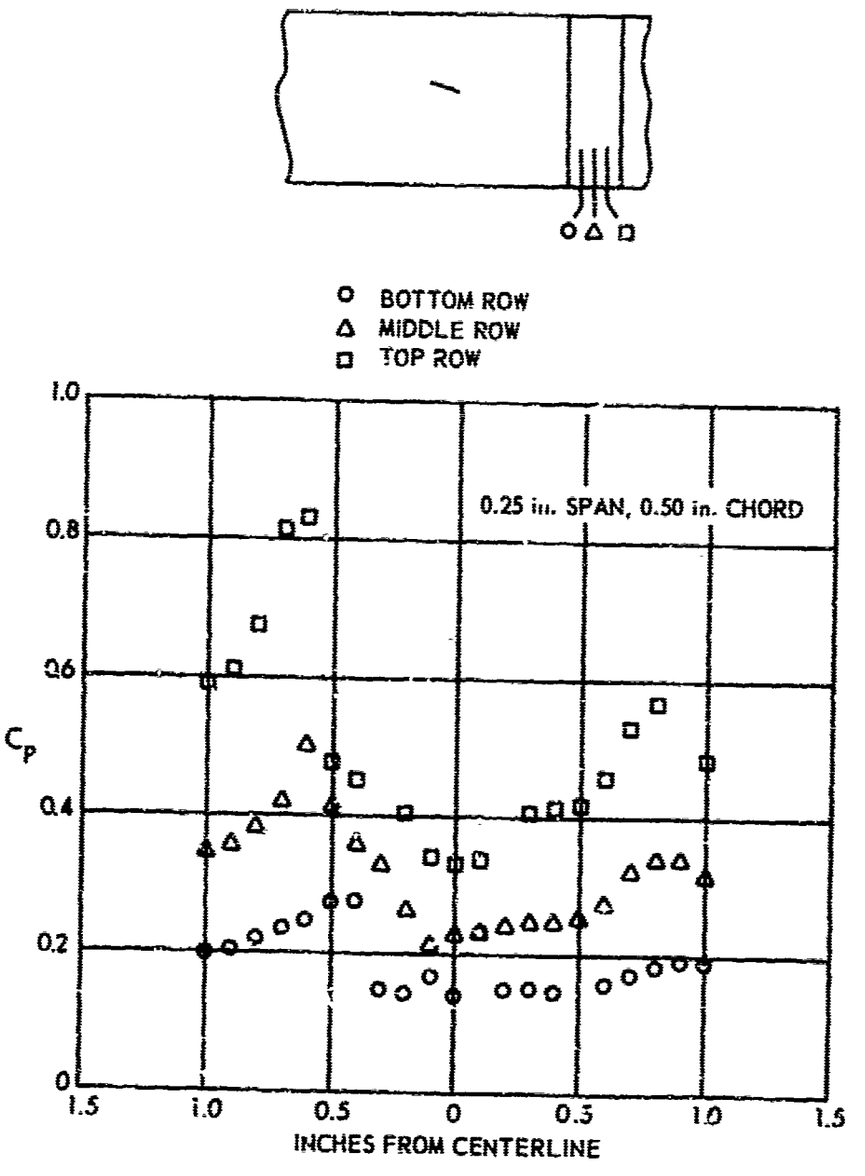

FIGURE 19b
SPANWISE PRESSURE COEFFICIENTS FOR
GENERATOR No. 3 IN AFT LEFT POSITION

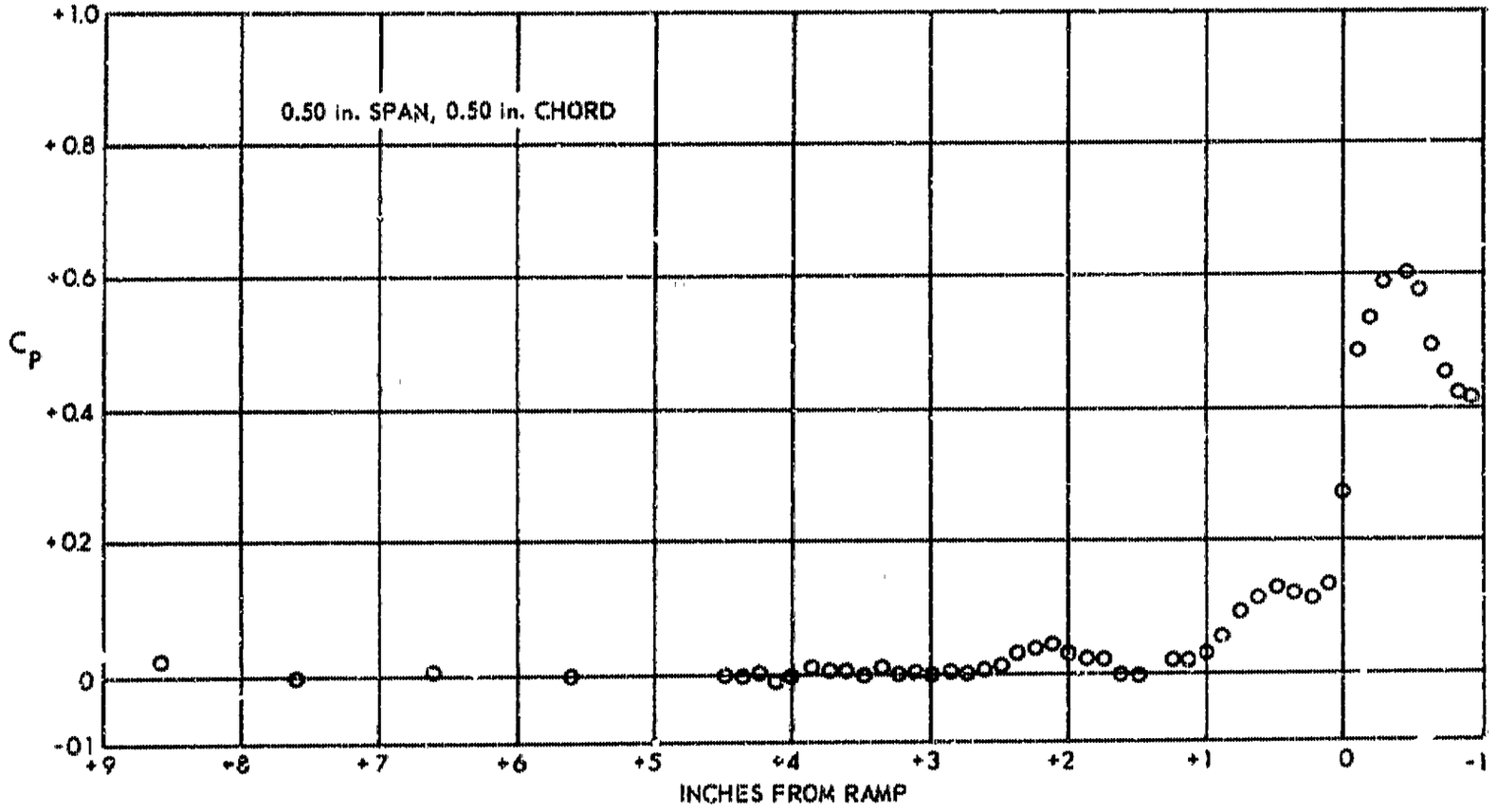

FIGURE 20a
CENTERLINE PRESSURE COEFFICIENTS FOR
GENERATOR No. 4 IN AFT LEFT POSITION

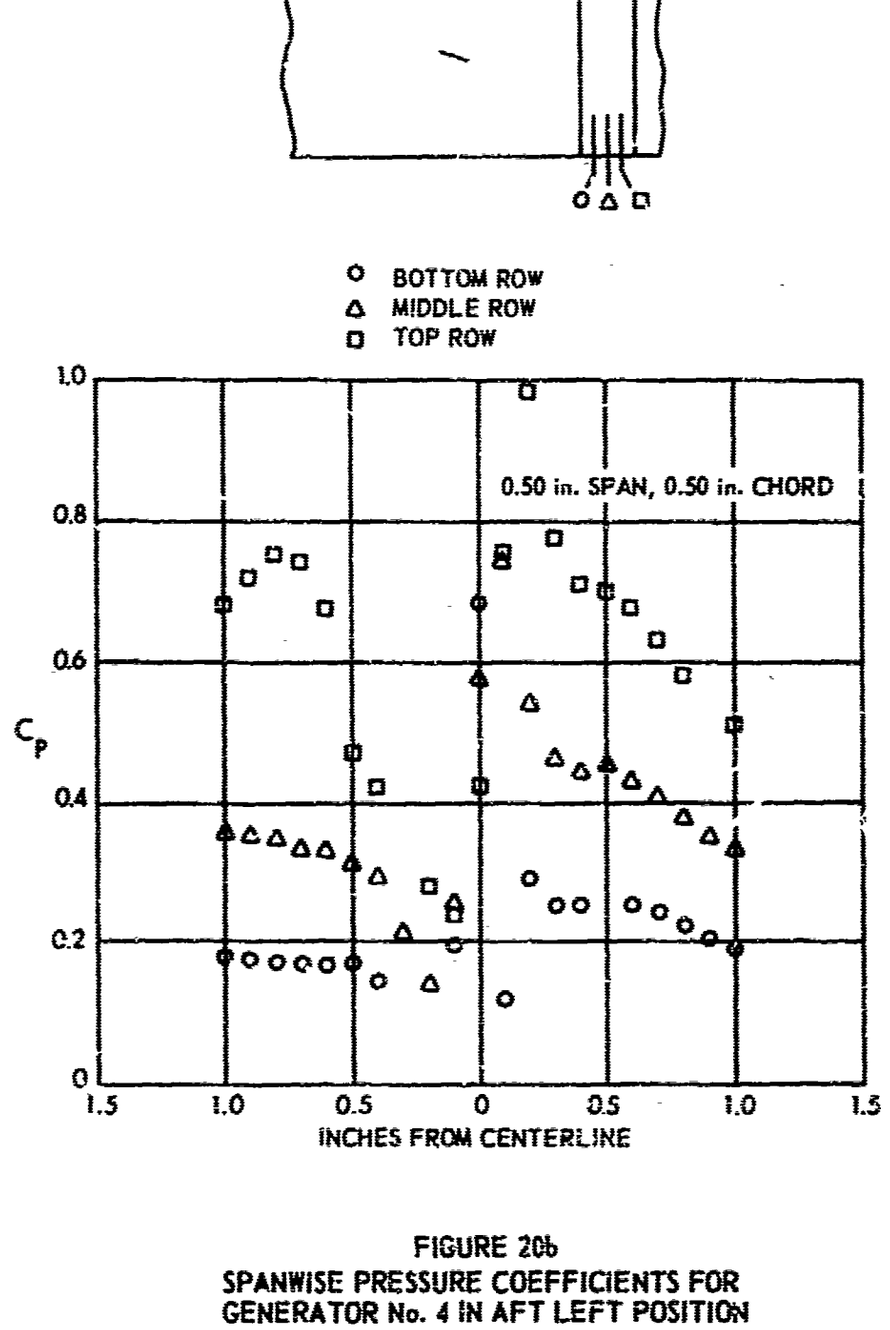

FIGURE 20b
SPANWISE PRESSURE COEFFICIENTS FOR
GENERATOR No. 4 IN AFT LEFT POSITION

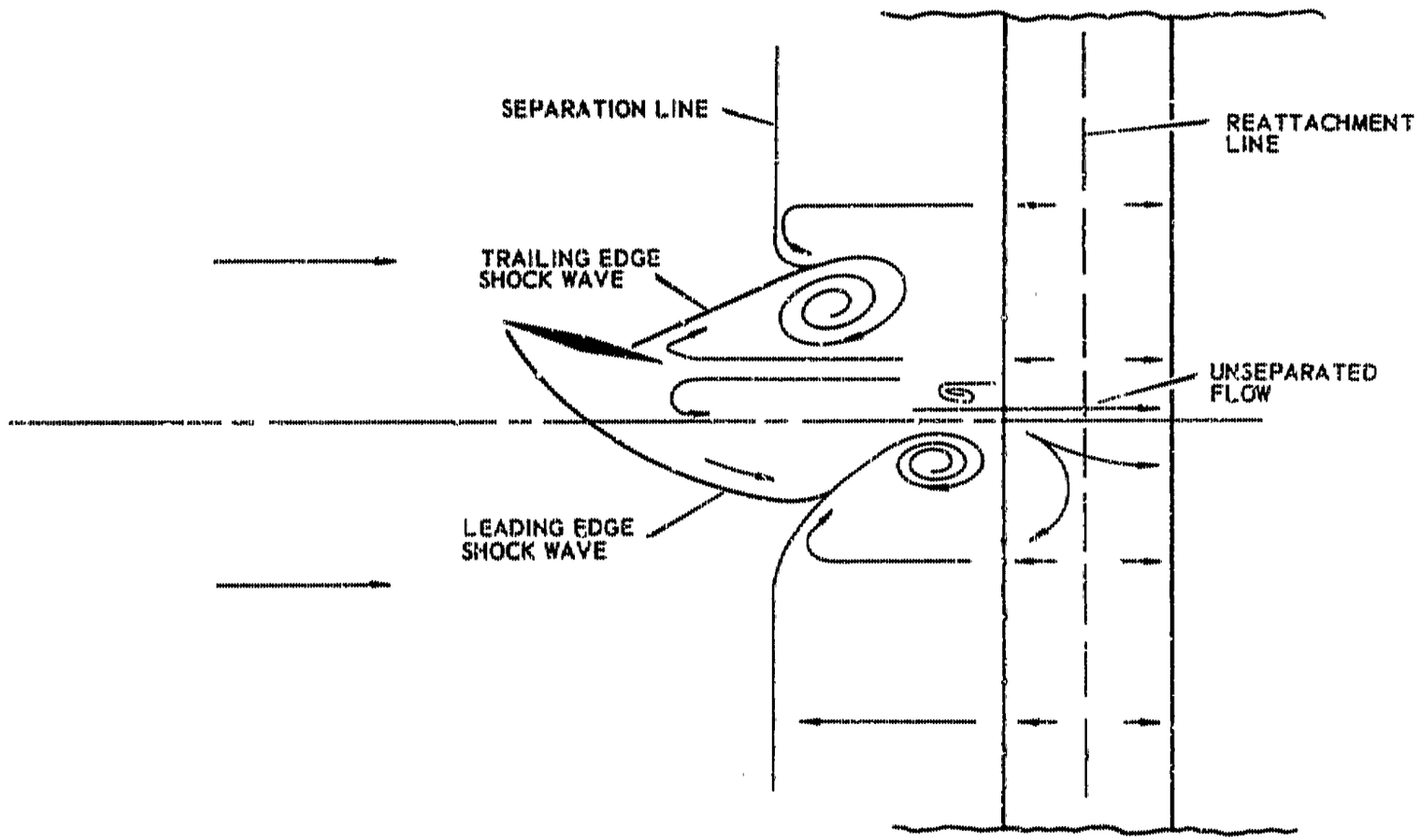

FIGURE 21
SKETCH OF OIL FLOW FOR
GENERATOR 1 IN AFT LEFT POSITION

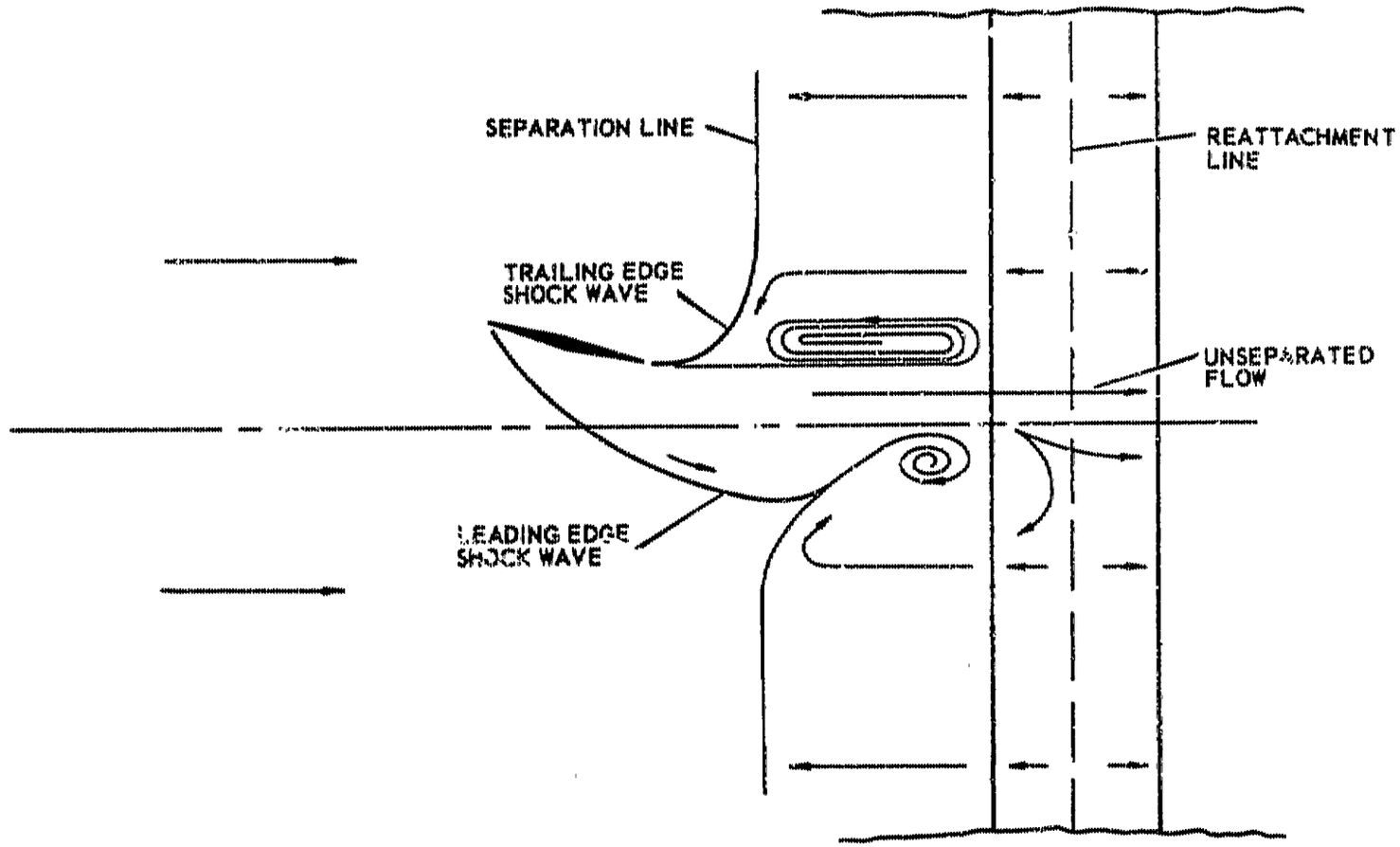

FIGURE 22
SKETCH OF OIL FLOW FOR
GENERATOR 2 IN AFT LEFT POSITION

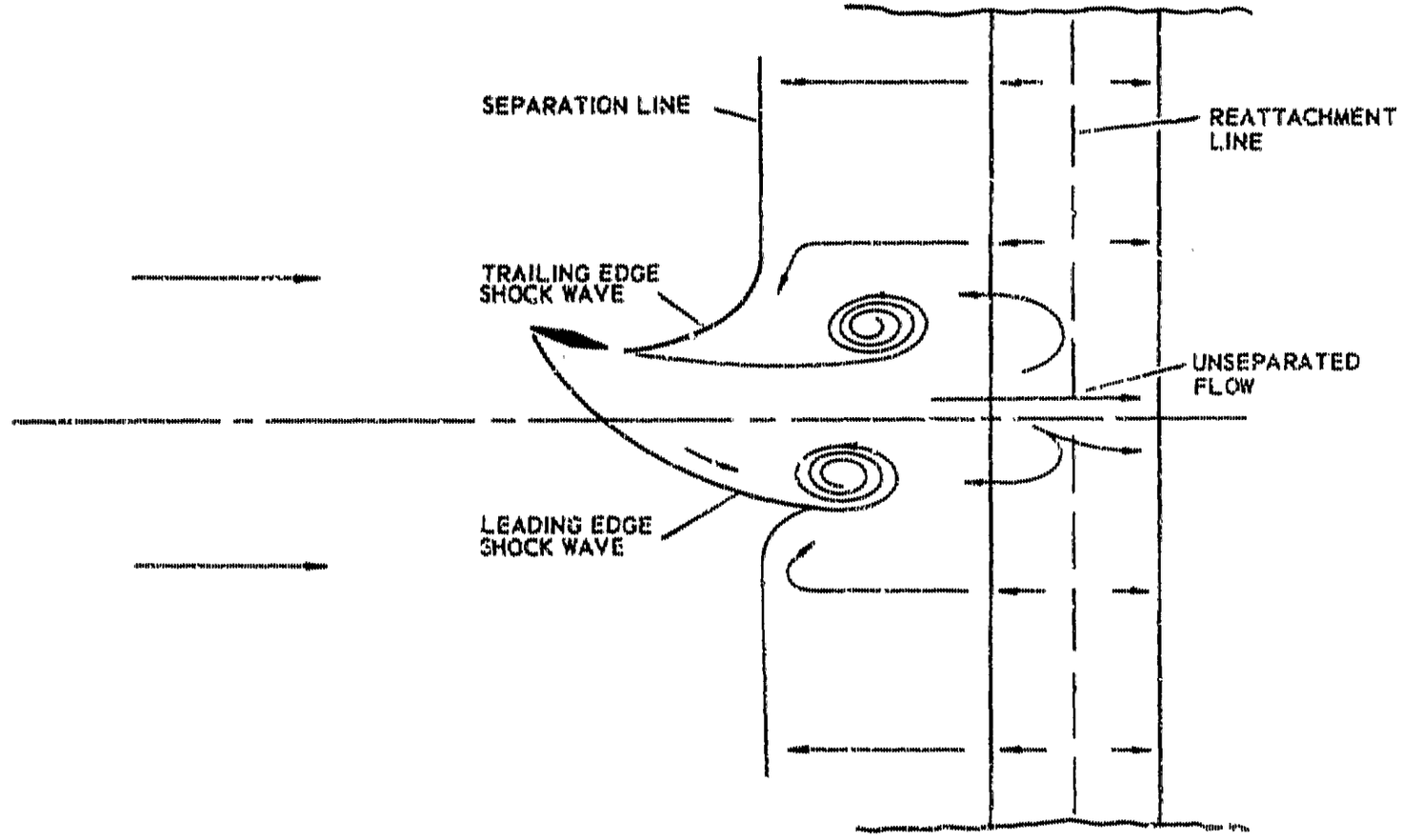

FIGURE 23
SKETCH OF OIL FLOW FOR
GENERATOR 3 IN AFT LEFT POSITION

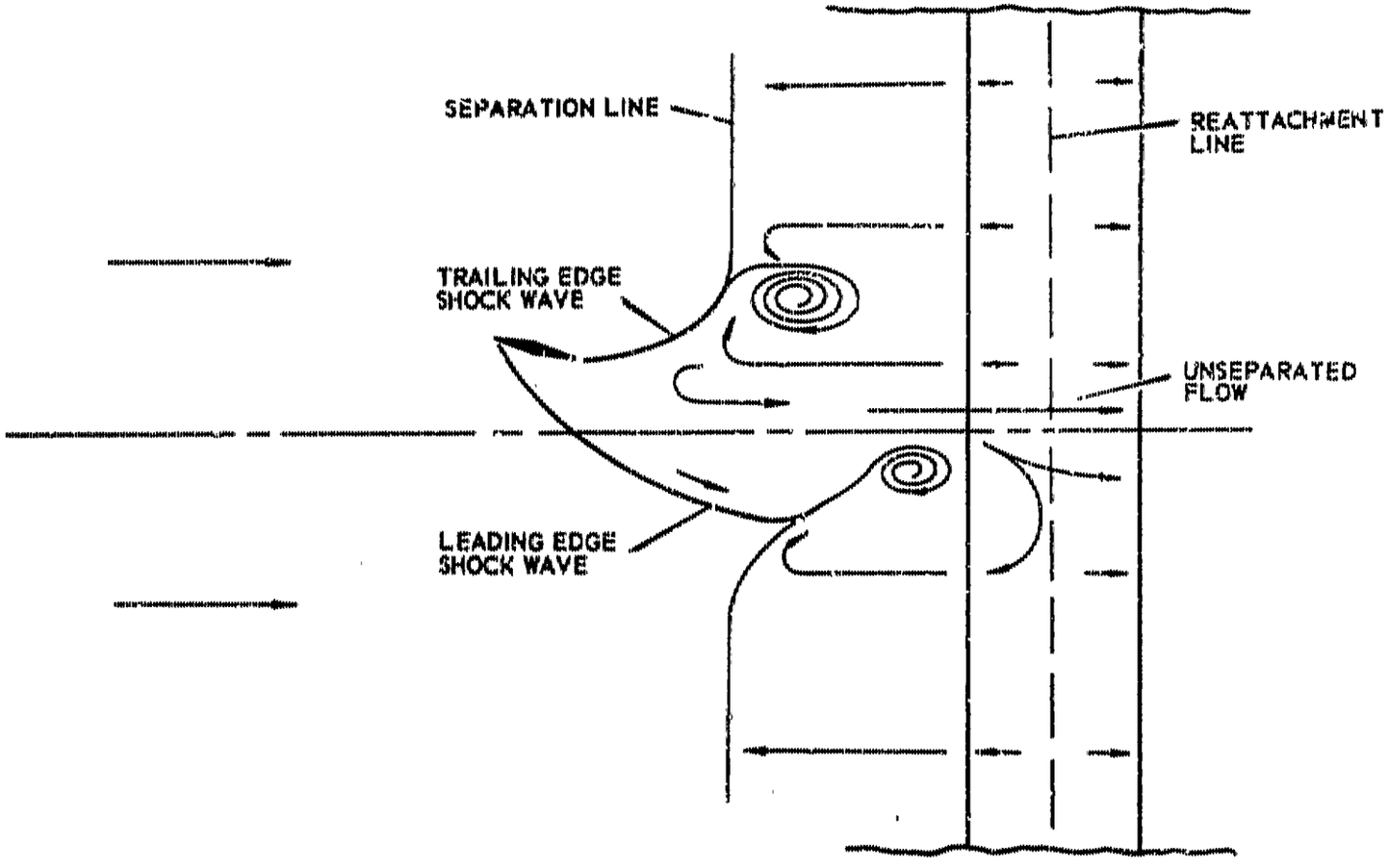

FIGURE 24
SKETCH OF OIL FLOW FOR
GENERATOR 4 IN AFT LEFT POSITION

FIGURE 26
SCHLIEREN PHOTOGRAPH OF COMPRESSION CORNER
WITH GENERATOR 1 IN AFT RIGHT POSITION